UNIVERSIDADE DE BRASÍLIA – UnB

INSTITUTO DE GEOCIÊNCIAS – IG

PROGRAMA DE PÓS-GRADUAÇÃO EM GEOLOGIA

CARACTERIZAÇÃO MINERALÓGICA E GEOQUÍMICA DE OCORRÊNCIAS DE ELEMENTOS TERRAS RARAS NO MACIÇO GRANÍTICO OURO FINO, RONDÔNIA, BRASIL.

DISSERTAÇÃO DE MESTRADO Nº 419

TIAGO BUCH

BRASÍLIA – DF

UNIVERSIDADE DE BRASÍLIA – UnB

INSTITUTO DE GEOCIÊNCIAS – IG

PROGRAMA DE PÓS-GRADUAÇÃO EM GEOLOGIA

CARACTERIZAÇÃO MINERALÓGICA E GEOQUÍMICA DE OCORRÊNCIAS DE ELEMENTOS TERRAS RARAS NO MACIÇO GRANÍTICO OURO FINO, RONDÔNIA, BRASIL.

TIAGO BUCH

Dissertação apresentada ao Programa de Pós-Graduação em Geologia do Instituto de Geociências, Universidade de Brasília como requisito para obtenção do título de Mestre em Geociências, área de concentração Geoquímica.

Orientador

Prof. Dr. Valmir da Silva Souza

Coorientador

Prof. Dr. Carlos Eduardo de Mesquita Barros

Banca Examinadora

_____

Prof. Dr. Valmir da Silva Souza (IG-UnB)

_____

Prof. Dr. Artur Cezar Bastos Neto (IG-UFRGS)

_____

Profª. Drª. Paola Ferreira Barbosa (IG-UnB)

BRASÍLIA – DF

2018

AGRADECIMENTOS

Eu agradeço à minha companheira e à minha família por me apoiarem e estarem comigo em todas as decisões e caminhos que tomei. Agradeço ao Prof. Carlos Eduardo por ter aceitado o desafio de fazer este projeto em uma região remota. Na memória do Prof. Bernhard, sou grato a ele por ter tornado este trabalho possível e ter insistido para que estudássemos a mineralização de Costa Marques. Gostaria muito que ele tivesse conosco.

Agradeço aos Professores Valmir e Nilson por dar todo o suporte na conclusão deste projeto.

Ainda, sou grato aos amigos José Roberto, Rodrigo A., Potato, Guilherme Ferreira, Cassiano Castro, Fucks, e Marcelo Esteves.

RESUMO

A mineralização em ETR da Suíte Intrusiva Ouro Fino permaneceu como um mero ponto de ocorrência mineral por décadas. Este trabalho é a primeira abordagem para estudar esta mineralização. Através de petrografia, geoquímica, química mineral e difração de raios X, este trabalho pôde abordar os principais aspectos geológicos e mineralógicos da Suíte Intrusiva Ouro Fino e relacionar a qual mineral estão constritos os ETR. Duas outras suítes intrusivas foram identificadas na região: Suíte Intrusiva São Domingos e Suíte Intrusiva Costa Marques. Os dados geoquímicos da Suíte Intrusiva Ouro Fino definem-na como peralcalina, de caráter alcalino a alcalino-cálcico, e claramente, um granito intraplaca de subtipo A2. Teores de óxido de elementos terras raras variaram de 0,47 a 1,65% nas amostras analisados, prevalecendo o enriquecimento dos ETRL em relação aos pesados ($La_n/Yb_n \approx 8$). Junto com os ETR, teores >10.000 ppm de Zr foram identificados nessas amostras. As análises de química mineral e petrografia identificaram dois zirconossilicatos portadores de ETR: elpidita e zircão. A elpidita é pervasiva em todas as amostras coletadas, atigindo até 5% da matriz, já o zircão ocorre ocupando pequenos interstícios da rocha. O zircão é o mineral que mais contém ETR em sua estrutura, com teores de óxido de elementos terras raras entre 3.2% e 7,4%. Nas análises químicas da elpidita, os teores totais de La2O3 + Ce2O3 + Y2O3 variaram de 0,21 a 1,92%. Como mineral acessório de ETR, há titanita, com teores de óxidos de ETR no intervalo entre 1,07% e 3,53%. Por serem zirconossilicatos, os zircões analisados contêm teores de Zr variando entre 56,1 e 59,8% e os cristais de elpidita, estão entre 18,9 e 21%. As suítes intrusivas à Suíte Intrusiva Ouro Fino não representaram nenhum tipo de influência à mineralização de ETR-Zr. Os dados petrográficos e de química mineral mostram um enriquecimento de sódio no sistema, marcado por bordas de reações no anfibólio e albitização moderada dos feldspatos potássicos. Este hidrotermalismo sódico gerou também enriquecimento de Ca em cristais primários de elpidita. O fracionamento de ETR se deve à incorporação dos mesmos na estrutura dos zirconossilicatos e posteriormente precipitação por decréscimo na temperatura do sistema. Deste modo, a mineralização da Suíte Intrusiva Ouro Fino caracteriza-se por um processo de autometassomatismo. Mineralizações de ETR-Zr em granitoides agpaíticos semelhantes à da Suíte Intrusiva Ouro Fino são encontradas nos depósitos de Khan Bogd, Khalzan Burgetey e Strange Lake.

TABLE OF CONTENTS

FIGURES INDEX

TABLES INDEX

1. INTRODUCTION

1.1. Presentation and Objectives

In accord to the IUPAC, the Rare Earth Elements group is composed of the 15 lanthanides together with Y and Sc. However, the inclusion of Sc in this concept is still not helpful, given the different behavior of Sc in nature (Wall, 2014). Also, the short-life of Pr makes this element exceptionally rare in nature, resulting in a group of 15 REE elements, composed of 14 lanthanides plus Y (Wall, 2014).

As a result of the increasing demand for REE in the global markets and the REE trade conditions imposed by China, the last decade became a period when several exploration projects for REE flourished (Paulick & Machacek, 2017). Among the deposits outside China, the main projects are in Canada, Brazil, Greenland and Austrália.

Brazil has currently eight deposits of REE, being two associated with granitic rocks and six with alkaline-carbonatite complexes (Takehara *et* al, 2016). The alkaline-carbonatite complexes sum a total of 261.3 Mt of ore with REE_2O_3 in a range from 0.7% up to 5.5%, as well the granitic REE deposits comprehend a total of 414 Mt of ore, being REE_2O_3 content equal or less than 1% (Takehara *et* al., 2016). The Rondonian Tin Province also contains in the stanniferours greisens with REE mineralization associated (Bettencourt, 1988 and 1991; Souza, 2003; Sparrenberger, 2002; Buch et al., 2016). However, information about the ore grades from these deposits is no quite precise. Among the REE ores associated with granites described by Takehara, the one from Costa Marques was the least known. The REE occurrence of Costa Marques is related to the Ouro Fino Intrusive Suite (Buch *et* al, 2018).

The existence of REE mineralization in the Ouro Fino Intrusive Suite (OFIS) is known since the project developed by Torres *et al*. (1978). After some mineral exploration follow-up made by Costa (1990) in the area, nothing had been developed in the region anymore. Because of the strong demand for REE, new sources for these elements must be explored. Therefore, some research to avail the potential of the OFIS for REE was required. This project is the first investigation to comprehend the mineralization of Costa Marques. The scope of this project comprises an integration of petrographic, petrological and mineralogical studies that aim to characterize the REE mineralization from the OFIS.

1.2. Location

The area of study locates in the southwestern border of the state of Rondônia with Bolívia. The reference city for support and logistic is Costa Marques. The access to Costa Marques is made from Porto Velho by the national highway BR-364 until the intersection with the national highway BR-429, that ends in the city of Costa Marques.

From Costa Marques to the study area, there are two entrances known as “km 22” and “km 26”. Counting from the city of Costa Marques, they respectively are 22 and 26 km away on the left side of the BR-429. The location of the study area is known in the region as Serra Grande Hill (Fig 1.1).

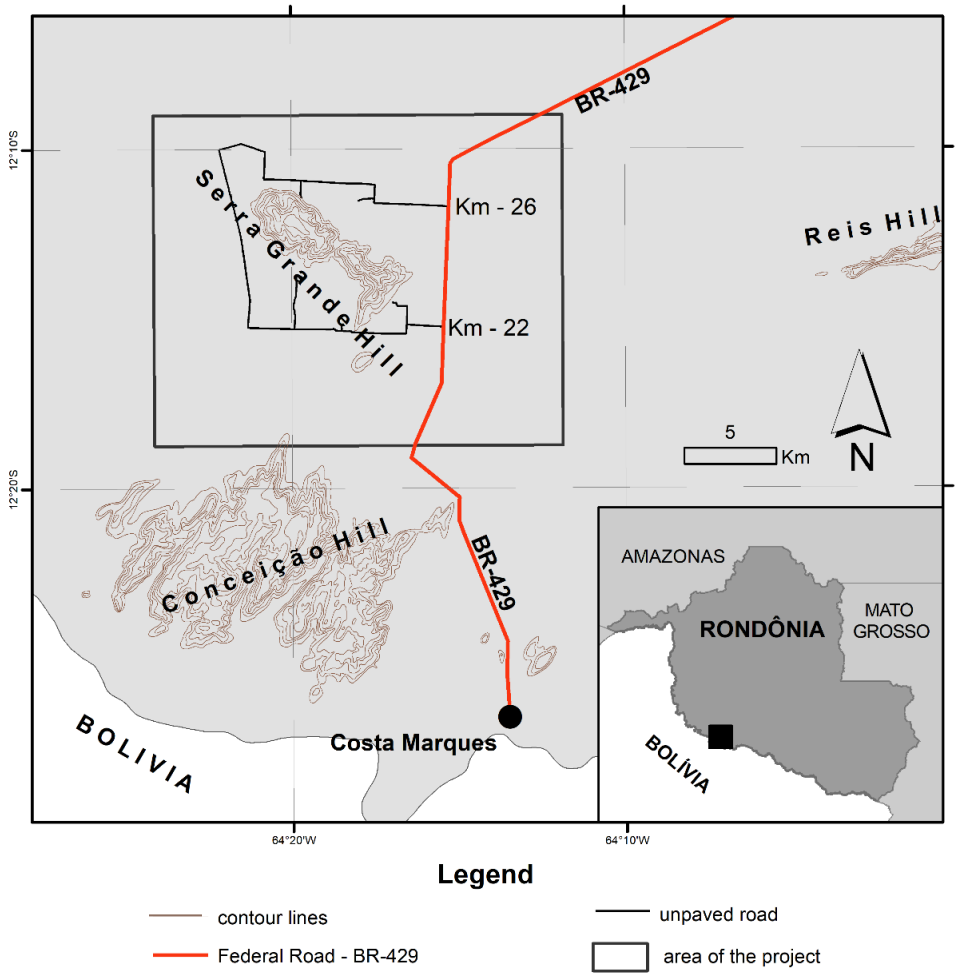

Figure 1.1: Planimetric location of the studied area. The area locates at the southwestern border of Rondonia with Bolivia. Main accesses to the Ouro Fino Inrusive Suiute domain are in the intersection of the federal road with the km-22 and km-26 entrances.

2. METHODOLOGY

2.1. Mapping and Sampling

For the studies of this project, a field survey was made in the area during the second half of July 2016, in the dry season. A total of 42 spots were described and 29 samples had been collected. The location of sampling spots is in Appendix 2.

The fieldwork data was compiled and interpreted in association with SRTM data provided by the National Institute of Space Research and geophysical data provided from the Geological Survey of Brazil (CPRM, 2010). The result of this interpration is a geological map in the 1:50,000 scale (Fig. 4.2).

2.2. Geochemistry

The chemical analyses for bulk-rock chemistry were executed by the ALS Global laboratory in Brazil. From the 29 collected samples, only 18 samples did not present to be weathered to be chemically analysed. In the set of analysed samples, 13 are from the Ouro Fino Intrusive Suite, 2 from the Sao Domingos Intrusive Suite and 3 from the Costa Marques Intrusive Suite. The location and type of the respective analysed samples are available in Table 8 of Appendix 2.

The techniques applied to analyse major elements and ICP-AES with preparation and for trace and rare earth elements, ICP-MS. Samples were analysed in laboratory ALS Global, using the Service Packs ME-ICP06 for ICP-AES and ME-MS81 for REE and trace elements. Samples for ICP-AES were prepared using funded lithium borate beads with acid digestion and for ICP-AES, the digestion was multiacid. More details about the analalytical proceeding can be found in the ALS-Global analytical schedule (ALS Global, 2018).

2.3. Rock powder X-Ray Diffraction

The samples CM-31 and CM-39 were assayed under the technique X-ray diffraction of rock powder. The analyses were performed by ALS Chemex laboratory using a Bruker D8 Focus Bragg-Brentano diffractometer with a tube of cobalt. The range of 2θ was between 2º and 70º, with a theta step size of 0.1º and an analysis speed of 1.2 s per step. The mineral composition was determined by the diffractometric results using the Rietveld method. The X-Ray Diffraction analyitical package to identify bulk-rock mineralogy in ALS Global is known as XRDSQ (ALS Global, 2018)

2.4. Mineral Chemistry

The mineral chemistry analysis had been made over thin sections of 8 samples from riebeckite-alkali feldspar granites. To identify the minerals that contain REE elements, the chosen technique is the electron microprobe analyzer (EPMA). Among the 8 samples, the samples were analyzed in the laboratory for electron microprobe analyzer from the German Geological Survey (BGR). The other 4 samples were analyzed in the laboratory for electron microbrobe of the Geosciences Institute of the University of Brasília (LME-IG).

The analyzed elements in the laboratory of electron microprobe of the BGR were Na, Mg, Al, Si, K, Ca, Ti, Mn, $Fe^{2+,}$ Fe^{3+}, Sr, Y, Zr, La, Ce, and Hf. The targeted minerals were amphiboles, pyroxenes, titanite, zircon, and elpidite. For the assays, a JEOL JXA-8530F was utilized. The analysis conditions occurred with a sample current of 40 nA and voltage acceleration of 20kV. The utilized lines are Kα – Na, Mg, Al, Si, Ca, Fe, and K with 10 s of peak measuring time; Kα – Ti, with 20 s of peak measuring time; Kα – Mn, with 30 s of peak measuring time; Lα – Sr and Y, 30 s of peak measuring time; Lα – Zr, with 60 s of measuring time; Lα – La, with 60 s of measuring time; Lα – Ce with 50 s of peak measuring time and; Lα – Hf, with 50 s of peak measuring time. The standards utilized were diopside (Mg and Ca); jadeite (Al, Si, Na), rutile (Ti), rhodonite (Mn), almandine (Fe), orthoclase (K), synthetic zirconia (Y, Hf), coelestine (Sr), zircon (Zr) and monazite (La, Ce).

In the LME-IG, the utilized device was a JEOL JXA-8230. For the analyses, three different proceedings were developed. One was specific for (i) major elements on amphiboles and pyroxenes, one was for (ii) major elements of potential REE minerals and the last, (iii) for REE elements on amphiboles, pyroxenes, and potential REE minerals.

- (i) for the pyroxenes and amphiboles, the analysed elements are F, Al, Si, Ca, K, Cl, Ti, Cr, Mn, Sr, Ni, Fe, V, and Ba. The assay utilized a sample current of 10 nA and voltage acceleration of 15 kV. The utilized lines are Kα – Na, F, Al, Si, Ca, K, Cl, Ti, Cr, Mn, Ni, Fe, and V; Lα – Ba, Sr.
- (ii) in the potential REE minerals, the analysed major elements are F, Al, Si, P, Nb, Mn, Ti, Y, Ta, Ca, Fe and Zr. The applied sample current was 10 nA and the voltage acceleration 15 kV. The employed lines for the elements are Kα – F, Al, Si, P, Mn, and Ti; Lα – Y; Kβ – Ca; and Lβ – Nb.

- (iii) in the assays for REE, Na, K, U, Th and Ba were analysed as well. The analyses were conducted with voltage acceleration of 20 kV and sample current of 50 nA. To analyse Na and K, the Kα line was utilized. Lantanium, Ce, Nd, Eu, Gd, Er, Tm, Yb, Lu and Ba were analised on the Lα line. For Ta, the applied line was Mα.

For the analyses on pyroxenes and amphiboles, the standards used are: albite (Na), forsterite (Mg), topaz (F), microcline (Al, K and Si), MnTiO3 (Mn and Ti), andradite (Ca and Fe), vanadinite (Cl and V), Cr2O3 (Cr), NiO (Ni), SrSO4 (Sr, BaSo4 (Ba).

In the analyses of REE minerals, the standards utilized in the assays are: topaz (F), microcline (Al, K and Si), apatite (P and Ca), LiNbO3 (Nb), MnTiO3 (Mn and Ti), YFe2O12 (Y), LiTaO3 (Ta), andradite (Fe), baddeyleite (Zr), albite (Na), vanadinite (Pb); ThO2 (Th), SrSO4 (Sr), CeO2 (Ce), UO2, BaSO4 (Ba). For for the REE, the glasses REE-1 (Eu, Gd, Tb, Tm), REE-2 (Sm, Nd, Yb, Lu), REE-3 (La and Pr) and REE-4 (Dy, Ho, Er).

The electron beam diameter was 1 µm, and the peak measuring time of 10 s in the peak and 5 s in the background.

3. SYNTHESIS OF REGIONAL GEOLOGY KNOWLEDGE

3.1. Geotectonic Context

The studied area situates at the extreme southwest border of the Amazonian Craton. In this region, the Amazonian Craton comprehends two geochronolocail provinces (Tassinari & Macambira, 1999). The former, is the Rondonian-San Ignacio, with ages between 1.55 to 1.3 Ga and the subsequent, is the Sunsás Province, with ages between 1.3 to 1.0 Ga. Accordingly to Bettencourt *et* al. (2010), the Rondonian-San Ignácio Province is bordered to the north and east by the Rio Negro-Juruena Province and to the south, is bounded by the Sunsás Province.

The Rondonian-San Ignacio Province comprises a geological set resulted from an orogeny involving the amalgamation of the Paraguá Terrane to other domains composed by the Rio Crespo Intrusive Suite (1.5 Ga), Rio Alegre Complex (1.51 – 1.48), Santa Helena batholith (1.45 – 1.42 Ga), Colorado Metamorphic Complex (1.36 – 1.3 Ga) and Pensamiento Granitoid Complex (1.36 – 1.30 Ga) (Cordani & Teixeira, 2007; Bettencourt *et* al., 2010) .

In accord with the map of Rizzotto et al., (2013) the Ouro Fino Intrusive Suite is inserted in the Guaporé Suture Zone (Fig. 3.1). The Guaporé Suture is the result of the amalgamation of the Paraguá Terrane with the Amazonian Craton (Rizzotto et al., (2013). The evolution of this suture zone included the generation of ultramafic magmatism followed the deformation of oceanic crust and supracrustal rocks and granitogeneses during the collisional phase (Rizzotto *et* al., 2013). The Trincheira Complex represents the ophiolitic crust formed between 1470 and 1435 Ma and the Colorado Metamorphic Complex is the supracrustal rocks group deposited over the Trincheira Complex. The metamorphism of the Colorado Metamorhic Complex took place around 1350 to 1330 Ma.

Occurying in the centre-north of Rondonia, the intrusive suites Santo Antônio (1,41 Ga), Teotônio (1.39 Ga), Alto Candeias (1.34 Ga) and São Lourenço-Caripunas (1.3 Ga) were associated to late to post-tectonic magmatism related to the Rondonian-San Ignacio (Bettencourt *et* al., 2010).

Within the Guaporé Suture Zone, Rizzotto (2010) present two intrusive suites of ages around 1.3 – 1.4 Ga. The Igarapé Enganado (1.36 Ga) and Alto Escondido (1.34) intrusive suites are the result of late to post-colisional magmatism inside the Guaporé Suture Zone. The plutonism of these suites is correlated to the plutonism resulted from the Rondonian-San Ignacio events in other regions of Rondonia (Gilmar José Rizzotto, 2010).

The Ouro Fino Intrusive Suite was only recently discovered (Bettencourt *et* al., 2012). For several years, the only dated magmatism in the studied area was from the Costa Marques Group, around 1.0 Ga (Torres *et* al., 1979). The magmatism of the Costa Marques Group was associated with the Sunsas Geochronoligical Province and correlate to the Rondonian Intrusive Suite, both result of post-collisional plutonism (Quadros & Rizzotto, 2007). Since new data have been presented, new interpreations are necessary to come. However, there is still no work interpreting the origin of the Ouro Fino Intrusive Suite magmatism face the regional deformatinal events of the Rondonian-San Ignacio Province.

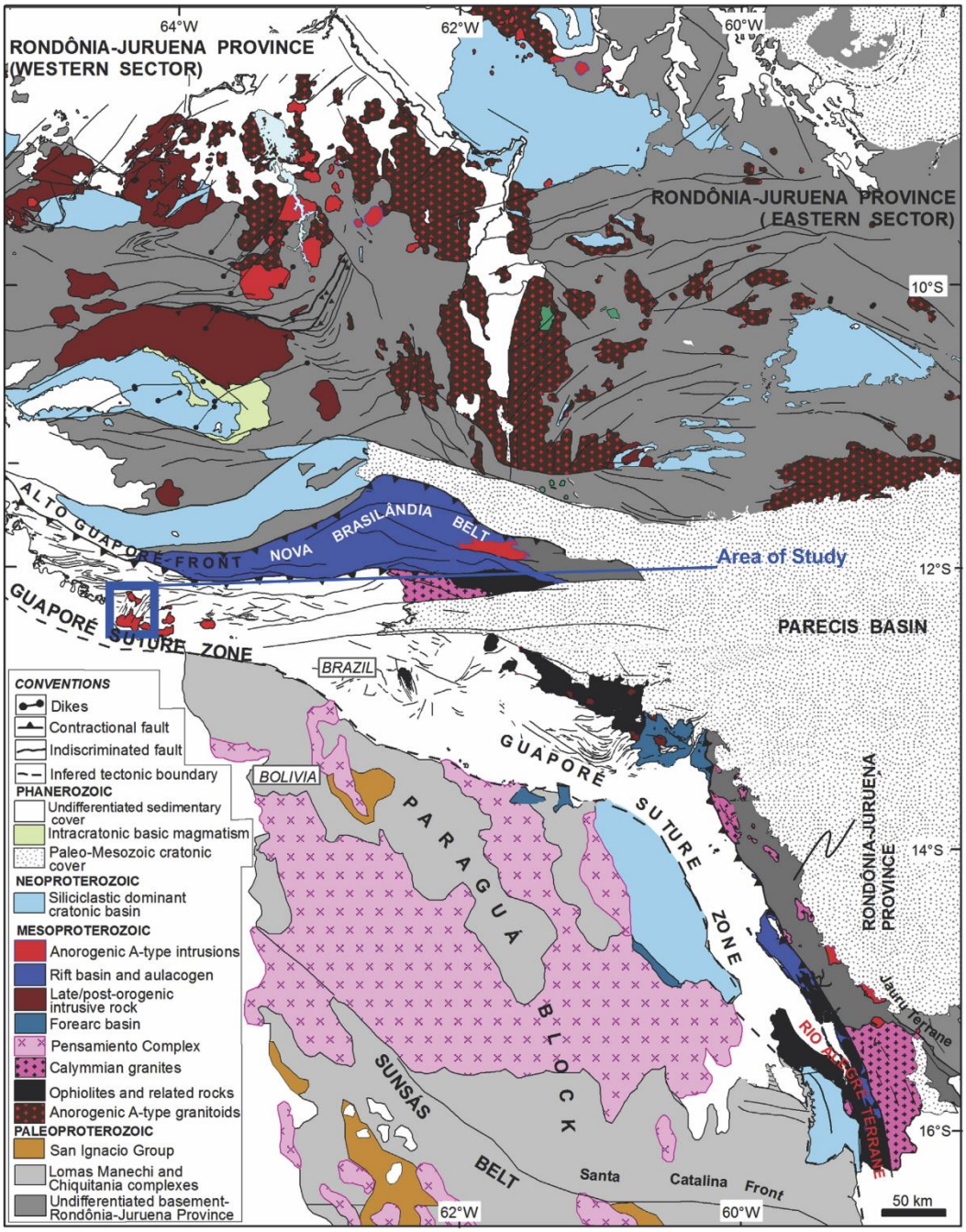

Figure 3.1: Location of the studied area in the regional geological context. The area is located within the Guaporé Suture Zone in accord to Rizzotto et al. (2013). Figure adapted from Rizzotto et al. (2013).

3.2. Previous Works

The first reports about the geology of the region were written by Lobato *et* al. (1966). Subsequently, the projects Southwest of Rondônia (Torres, 1979) and the RADAM Brasil – Quadricule Guaporé SD.20 (Santos *et* al., 1979) developed recognisement studies in the region. The former was on 1:500,000 scale and the last, 1: 1,000,000.

During the 1980's, the Geological Survey of Brazil, formely called CPRM, developed studies to identify areas with metalogenetic potential (Freitas *et* al., 1985). Afterwards, Costa (1990) developed an exploration survey for REE in the Serra Grande Hill, which is the work that identifies the potential for REE in the Serra Grande Hill.

Other studies improved the knowledge about the geological background in the area (Scandolara,1999; Rizzotto *et* al., 2004; Quadros & Rizzotto, 2007). However, these works were developed on a regional scale and did not discuss specifically the granitic rocks from the southwestern border of Rondonia State.

Not long ago, Bettencourt *et* al. (2012) redefined the framework of the granites from Costa Marques. As well other further studies regarding the lithogeochemistry and Hf-isotopes geochemistry of granites from Costa Marques were published recently (PayollaI *et* al., 2013; Bettencourt *et* al., 2014).

3.3. Regional Geology

Initially, the most ancient rocks in the region were defined by Torres et al. (1979) and Santos et al. (1979). However, the following studies on the regional background of Scandolara (1999) and Quadros & Rizzotto (2007) contradicted the proposed ages and tectonic events that occurred in this region at the beginning and end of the Neoproterozoic.

With the airborne geophysical surveys contracted by the CPRM and the geochronological analyzes published in other articles, it became possible to advance the understanding of the tectonic limits in the studied region. In this way, the units will be described in the sequence of the most recent stratigraphy, but the older terms will be mentioned since the basement rocks in this part of the state of Rondônia still need more detailed geochronological studies.

3.3.1. Colorado Metamorphic Complex

The Colorado Metamorphic Complex (CMC) is an association of metavulcanosedimentary rocks by Rizzotto et al. (2007) near Colorado do Oeste - RO. According to the authors, this association of rocks is subdivided into four lithophacities: Metapelitic Unit, Metapsytic Unit, Iron-Manganese Unit and Calcissilictic Unit. The existence of these rocks as a basement of the studied area is defined by Quadros & Rizzotto (2007) and was defined through the interpretation of tectonic limits interpreted from

aerogeophysical data. Torres et al. (1979) called the metamorphic rocks intruded by the former Costa Marques Complex as Serra dos Reis Unit. Hence, in order to seek a concordance that eliminates this hiatus on the geological knowledge, the subdivisions of the Colorado Complex defined by Rizzotto et al. 2007) will be described and followed by the Serra dos Reis Unit mentioned by Torres et al. (1979). According to Rizzotto et al. (2007), the CMC rocks were formed in a regional metamorphic event, of medium amphibolite facies

3.3.1.1. Metapelitic Unity

The metapelitic unit of the Colorado Metamorphic Complex is formed by elongated and sigmoidal lenses of metric length or, that could reach up to 25 km. The lithotypes that compose it are muscovite-biotite-quartz schists, granada-silimanite-biotite schists, silimanite-staurolite-biotite schists, silimanite-staurolite-biotite-quartz schists and locally, graphite-schists. Cutting these rocks, there are veins of quartz with blasts of subhedral muscovite.

The fabric of these rocks contrives a crenulated schistosity, indicating at least two deformations. The mesoscopic-scale crenulations are indicated by isoclinal and intrafolial folds, with or without roots.

Hosted in these rocks, there are pockets of granitic composition (neosomas) parallel to sigmoid schistosity. Porphyroblasts of aluminous minerals such as grenade and subordinately staurolite are common and have their origin possibly associated with contact metamorphism. As well, there are porphyroblasts of grenade parallell to the main foliation.

3.3.1.2. Metapsamitic Unity

This unit is composed by migmatitic gneisses and occurs interbedded with the metapelitics and paraderivated units. The migmatization is indicated by pods and lenses of granitic leucosoma (neosoma). The neosome lenses are concordant with the banding/foliation of gneisses. The petrography indicates that the origins of these gneisses are from pure and impure sandstones (metarkoses). The sillimanite and cordierite of these rocks indicate high grade metamorphism.

The felsic layers vary between 1.0 and 1.5 mm in thickness and the mafic layers vary between 1.0 and 3.0 mm. These layers have isoclinal and intrafolial folds with root,

defined by the folding of aggregates of biotite and sillimanite; thus indicating at least two deformations.

3.3.1.3. Ferro-Manganesiferous Unity

The occurrence of this unit is irregular and discontinuous. The foliation is parallel to the foliation of the units mentioned above. This unit is composed of layers of metacherts intercalated with layers of iron and manganese oxides. Among these layers, there may be amphibolites, schists and associated paragneisses. The most frequent lithotypes are magnetite-metachert, hematite-quartzite and ferruginous quartzite. These layers of silica and oxides of iron and manganese have thicknesses ranging from millimeters to centimeters.

3.3.1.4. Calcissilicatic Unity

Discontinuous lenses of calcissilicatic gneiss are generally intercalated with amphibolites. They have a constricted to the extreme northwest of Pimenteiras city. The constituent minerals are diopside, plagioclase, quartz and, to a lesser extent, granade. These minerals are segregated in layers of millimetric thickness, defining the foliation of the rock.

3.3.1.5. Paramphibolite Unity

This unit is associated with calcissilictic gneisses and occurs as narrow and elongated layers of very local occurrence. It is dark gray in color and fine grained. The fabric is composed of centimetri-decimetric layers of amphibole texture nematoblastic cut by quartz venules parallel to the foliation. According to Rizzotto et al. (2007), the CMC rocks were formed in a regional metamorphic event, of medium amphibolite facies.

3.3.1.6. The Serra dos Reis Unity

As mentioned previously, Quadros & Rizzotto (2007) defined the Colorado Metamorphic Complex as the country rock for the granites of Costa Marques. Concordant to these authors, the Colorado Metamorphc Complex is the same group of metamorphic rocks denominated Serra dos Reis Unity, by Torres et al. (1978).

Torres describes the Serra dos Reis Unity as na elongated hill striking E-W, at NE of Costa Marques city. It occurs also as inselbergs in the Guaporé River's flood plain.

The Serra dos Reis Unity is formed byt metarenites, metarkoses, and quartzites. Locally, there are conglomeratic meta-arkoses, fine-grained metarenites and purple phylites (Torres et al., 1979).

Torres *et* al. suggest the probable age for the Serra dos Reis Unity is between 1.8 and 1.5 Ga. However, Scandolara (1999) infers that the Serra dos Reis Unity could be part of the Nova Brasilândia Metavolcanosedimentary Sequence, with age of 1.177±33 Ma (Rb/Sr bulk rock). In accord with Rizzotto *et* al. (2010), the Colorado Metamorphic Complex has ages between 1312±3Ma and 1303±2Ma (Ar/Ar in biotite of anatexites).

For the description of the Colorado Metamorphic Complex and its correlate Serra dos Reis Unity, its assumed that the Serra dos Reis Unity corresponds to the metapsamitic unity of Rizzotto *et* al. (2007).

3.3.2. Costa Marques Complex: three alkaline intrusive suítes

The first mention of Costa Marques granites was made by Lobato et al. (1966), while reporting rocks near the Príncipe da Beira Fortress The authors describe rocks with porphyritic texture and probably mineralized to cassiterite. Santos et al. (1978) define as Costa Marques Group porphyritic granites and as well, rhyolites, andesites, tufts, porphyry quartz, granites and granophyres, that appear near the homonymous region. According to these authors, "lithotypes are extremely differentiated going mainly from acid to intermediate, as well as some mafic local exposures. Santos *et* al. (1978) reportes the most complete description of the rocks associate to the Costa Marques Group, which is summarized below:

3.3.2.1. Granites

Granites are the most abundant lithotypes in the Costa Marques Group. They are of phaneritic texture, generally medium to coarse grained, sometimes porphyritic. The granites present brown, pink and gray coloration, and sometimes presenting dark or greenish spots and a leucocratic color index.

In micropetrography, there is micropertitic intergrowth in the feldspars (hypersolvus). The habit of these crystals is anhedral to subhedral, occurring Albite or Carlsbad twinnings. The quartz crystals are of anhedral, with fractured edges, and sometimes with undulating

extinction. Myrmequite intergrowth between quartz crystals and feldspars is another common feature.

The biotite crystals vary from green to brown, with strong pleochroism. These crystals are distributed in lamellae and replace the hornblende. Inclusions of zircon are rare.

The amphibole occurs in two varieties, hornblende and biotite. The hornblende is of tabular form, with euhedral crystals. Riebeckite occurs as tabular crystals or sub-radiated aggregates of very small prisms. These crystals are intensely pleochroic, with the color varying from dark blue to yellowish green. Other minerals that make up the rock are opaque and titanite anhedral, zircon in tiny euhedral prisms, fluorite, alannite in more developed euhedral crystals and apatite. As altering minerals occupying mainly fractures, there are sericite, leucoxene, clay-minerals, chlorite, epidote-zoisite and iron oxides.

3.3.2.2. Granophyres

In accord to Santos *et* al. (1978), the granophyres are rocks with "pinkish-gray" coloration, porphyritic texture with a microphaneritic matrix. The rock has a massive structure and is consisted essentially of quartz, feldspar, epidote or mafic mineralss.

Under the microscope, not all the samples studied by these authors revealed phenocrysts. These samples without phenocrysts showed a microfaneritic texture, with an incipient finer granulation than porphyritic granophyres. Feldspar phenocrysts can reach 2.5 cm length and form clusters resulting in a glomeroporphyrytic texture. Opaque minerals are abundant and appear as altered or disseminated mineral clusters in the matrix. As accessory minerals, there are apatite and zircon in the form of small euhedral crystals. Rarely, there is biotite, which is sometimes chloritized.

The alteration minerals are chlorite and epidote. The chlorite occurs in the form of lamellar and fibrorradial aggregates; and the epidote in small crystal agglomerates.

3.3.2.3. Syenytes

Syenites are scarce in the Costa Marques Group. They are coloured brown, medium-coarse grained, and are essentially composed of orthoclase, microcline, plagioclase and hornblende. In micropetrography, it is possible to observe cataclastic deformation in the crystals with undulating extinction, marginal microgranulation (generation of subgrains), curved geminations and mineral comminution with faceted subgrains.

3.3.2.4. Rhyolites

Rhyolites are of reddish-brown to yellow-brown coloration, with fine granulation, porphyritic texture with matrix varying from aphanitic to microphaneritic. The constituent minerals are mainly quartz and K-feldspar.

In micropetrography, phenocrysts of feldspar and quartz vary from anhedral to euhedral are surrounded by a spherulitic matrix composed of feldspar and fibroradiated cristobalite. In the matrix, there are also opaque minerals, epidote and chlorite. The quartz phenocrystalls present corroded edges. Feldspars present Albite and Carlsbad twinnings. Perttitic intergrowth is observed as a result of the occurrence of plagioclase associated with potassic feldspar. As accessory minerals, there are zircon and titanite.

3.3.2.5. Rhyodacites and tuffs

These rocks are the most abundant of the Costa Marques Group, in accord to Santos *et* al. (1978). The rhyodacites present greenish gray colours, with porphyritic texture, aphanitic matrix and massive structure.

Under the microscope, the phenocrystalls are mostly feldspar (microcline and plagioclase) and subordinately, clinopyroxene. These phenocrysts are immersed in a fine-grained matrix composed essentially of quartz and feldspars. In addition, the matrix is also composed of chlorite, epidote, opaque minerals and more rarely, volcanic glass. When associated with K-feldspar, plagioclase occurs micropertitic intergrowth.

The clinopyroxene phenocrystalls are anhedrical sometimes altered to epidote or chlorite. Quartz crystals form an intergrowth with the feldspars. Eventually, there is still cryptocrystalline silica in the form of spherulites also associated with feldspars. Opaque minerals are quite numerous, in the form of tiny disseminated crystals or aggregates. Titanite, zircon and apatite are in trace quantities. Chlorite and epidote occur in large amounts possibly resulted from alteration processes.

The rhyodacitic tuff under naked eye is a rock of dark gray color, porphyritic texture and aphanitic matrix with massive structure. Its main constituents are mafic minerals, feldspar and quartz. In the microscope, there are fragments of basaltic rock and phenocrysts of quartz and feldspar. The matrix consists of feldspar, quartz and volcanic glass.

3.3.2.6. Trachytes

The trachytes exhibit gray color, with porphyritic texture and aphanitic matrix. Are composed essentially by mafic minerals and K-feldpsar. In microscopic scale, the K-feldspar (orthoclase), is scattered in the matrix beside aegirine crystals. The main phenocrysts are the orthoclase with pertitic intergrowth. As for accessories, the rock presents opaque minerals, zircon, titanite, quartz and apatite.

3.3.2.7. Andesites

Quite common, in the Group Costa Marques, the andesites prevail over leucoandesitos. The color varies from pink to dark gray, and the colour index varies from leucocratic to melanocratic. The texture is usually unequigranular, with aphanitic matrix and feldspar phenocrysts. Less frequent are the rocks with aphanitic or fine phaneritic textures. The main constituent minerals are plagioclase, biotite and amphibole.

In the micropetrography, feldspars are predominantly identified as plagioclase, which is moderately sericitized, with antipertitites, subhedral habit, and Albite and Carlsbad-type geminations. The identified member of the plagioclase series is andesine. In the matrix there is also chlorite, resulted from the biotite and hornblende alteration. Quartz when observed, is of anhedral habit and undulating extinction. Minerals identified accessories are opaque minerals, zircon, apatite, titanite, epitope and subordinately rutile.

3.3.2.8. Reclassifications and Geological Knowledge Update

After Santos *et* al. (1978), Torres et al. (1978) defined the Costa Marques Group as Costa Marques Complex, a denomination that has been preserved until the work of Bettencourt et al. (2012). These authors subdivided the Costa Marques Complex into three distinct magmatic suites: two plutonic and one subvolcanic. Concordant to Bettencourt et al. (2012), the first plutonic suite contrives gray aegirina-augita-riebeckita quartz-syenites and alkali-feldspar granites. The second plutonic suite characterized by Bettencourt et al. (2012) is composed of pink-coloured hornblende-biotite sienogranites with medium to coarse granulation and porphyritic or seriate textures and, gray biotite alkali-feldspar granites of fine-medium granulation. Still, according to those authors, the subvolcanic suite features hornblende-porphyrus porphyry and hornblende porphyry rhyolites, with banded or massive structures.

These suites were named by Bettencourt et al. (2012) as Intrusive Suite São Domingos, Ouro Fino Intrusive Suite, with the concept of Costa Marques Suites, just a sub-suite. Payolla et al. (2013) classified these suites as alkaline-alkali suites, alkaline to metaluminous, and sodium and potassium affinity. According to these authors, the intrusive suites have geochemical characteristics of A-type granites.

The first ages of the Costa Marques Group were obtained by Santos et al. (1979), as providing an isochron of Rb/Sr with an age of 962 ± 72 Ma, in bulk rock analysis. This age off the Costa Marques Group to be correlated to the magmatism of the Rondônia Intrusive Suite. Much later, Bettencourt et al. (2012) analyzed U/Pb in zircons through SHRIMP technique and obtained three distinct ages, what resulted in the discrimination of three magmatic suites of the region. These authors conclude that the Ouro Fino Intrusive Suite is the earliest, with 1347 ± 9Ma. The São Domingos Intrusive Suite is the subsequent magmatism with an age of 1057 ± 10 Ma and, lastly, the Costa Marques Intrusive Suite with an age of 998 ± 10 Ma.

3.3.3. Guaporé Formation

Although of wide extension (Quadros & Rizzotto, 2007), the Cenozoic sedimentary and lateritic covers are little discriminated against each other in previous studies. In general, the cenozoic covers are associated with the geomorphological landscape of the Guaporé River Valley. The Guaporé Formation comprises unconsolidated sediments deposited in the alluvial plain of the homonymous river (Figueiredo et al.,1974, apud Santos et al., 1978). These authors correlate the Guaporé Formation with the Pantanal Formation, in the state of Mato Grosso, and divide it into two subtypes: lower and higher.

The lower level is determined as "unconsolidated lateritized clayish-arenous sediments" that occur in the non-flooded part of the plain. However, Torres et al. (1978) observed that the lateritization processes are much more prominent and describe ferruginous crusts with thicknesses ranging from 4 to 40 meters. These laterites are generally with continuous horizons with concretionary and/or pisolithic matrix.

The upper layer comprises the layers of sediment still depositing at the adjacent to the Guaporé River rails and its tributaries channels. According to Torres et al. (1978), this upper layers form terraces on the banks of the rivers of the region, or islands or sand banks. These authors observe that the types of sediments are variable, existing clay with or without

organic matter to coarse gravel. These characteristics are typical of meandering river environments.

Torres et al. (1978) propose a more consistent discrimination by differentiating the upper level in two groups of sedimentary deposits. The first group consists only of alluvial and fluvial sedimentary deposits associated with the banks and beds of the perennial rivers of the region. The second is related to eluvio-coluvial sediments, resulting from the lateral erosion of the escarpments of the Uopianes Hills, at the north of the studied area.

4. **SCIENTIFIC PAPER**

Petrological and mineralogical investigation on the Ouro Fino Intrusive Suite: a potential REE-Zr deposit in the southwest of Amazonian Craton, Western Brazil

Tiago Buch[a, *], Berhnard Manfred Bühn[b] (*in memorian*); Valmir da Silva Souza[b], Nilson Francischini Botelho[b]; Carlos Eduardo de Mesquita Barros[c]; Simon Goldmann[d].

a: Serviço Geológico do Brasil, 76801-581 Porto Velho – RO – Brazil.

b: Instituto de Geociências, Universidade de Brasília - UnB, 70910-900 Brasília, DF, Brazil

c: Departamento de Geologia, Universidade Federal do Paraná - UFPR, 81270-460 Curitiba, PR, Brazil.

d: Bundesanstalt für Geowissenschaften und Rohstoffe, D-30631 Hannover, Germany

Corresponding author:

Tiago Buch, email: tiago.buch@cprm.gov.br, phone: +55 69 3901 3700

Co-authors:

Valmir de Silva Souza, email: vsouza@unb.br

Nilson Francischini Botelho, email: nilsonfb@unb.br

Carlos Eduardo de Mesquita Barros, email: cadubarros@ufpr.br

Simon Goldmann, email: simon.goldmann@bgr.bund.de

4.1. Abstract

The alkaline granites of the southwest of southwest Rondonia, Brazil are known for high concentrations of REE. This study is the first approach to understand the REE mineralization of the Ouro Fino Intrusive Suite. This suite is composed of a hypersolvus peralkaline alkali feldspar granite. The mafic minerals are essentially sodic amphiboles and pyroxenes. Petrographical results indicate little mineralogical variation within the alkali feldspar granites. Associated with the Ouro Fino Intrusive Suite, late-magmatic alkali-rhyolite dykes occur. Unexpectedly, other plutonic rocks from Costa Marques and São Domingos intrusive suites occur in the studied local. The geochemical data identified total rare earth contents in the whole rock ranging from 0.47 up to 1.65%, and average $La_n/Yb_n \approx 8$. Also, high contents of Zr were identified in all the samples, eventually exceeding the upper limit of detection. The mineral chemistry results in EPMA identified zircon and elpidite as the main carriers of Zr and REE, and subordinately, titanite. The borders of amphiboles are rimmed by aegirine. As well, small crystals of Na-plagioclase formed on the edges of microcline crystals, which suggests that late magmatic processes occurred. The elpidite is considered as one of the minerals that incorporated Ca ions during hydrothermal-deuteric processes. Zircon crystals show a mantle of amorphous cryptocrystalline mass rich in REE. The other intrusive suites that occur in the area presented no characteristic that could be regarded to the mineralization. The REE-Zr mineralization is considered as a result of late-magmatic hydrothermal metasomatism followed by the cooling of the hydrothermal system. The incorporation of REE in the lattice of zirconsilicates is the main concentration factor as well, as REE concentrated by precipitation in the interstices of the rock. The REE-Zr mineralization of the Ouro Fino Intrusive Suites present mineralogical and petrological characteristics similar to the Strange Lake and Khan Bogd deposits.

Keywords: Zirconosilicates; peralkaline granites; REE; Rondonia; Amazonian Craton.

4.2. Introduction

In the last 25 years, the importance of rare-earth elements (REE) staggered. Being essential to the technology industry, the REE deposits became strategic, which resulted in a rush for new deposits. Several deposits of REE have been associated with alkaline granites and within-plate geological setting (Wall, 2014; Dostal *et* al, 2017; Chakhmouradian and Zaitsev, 2012). The Rondônia State, in western Brazil, hosts several REE-anomalous alkaline granitic suites, which may contain Sn, W, Nb-Ta and F mineralization and gemstones (Isotta et al. 1978, Betencourt et al. 1999, Quadros and Rizzotto, 2007). The Ouro Fino Intrusive Suite is located on the southwest side of the Rondônia State, very close to the border between Brazil and Bolivia (Fig. 4.1).

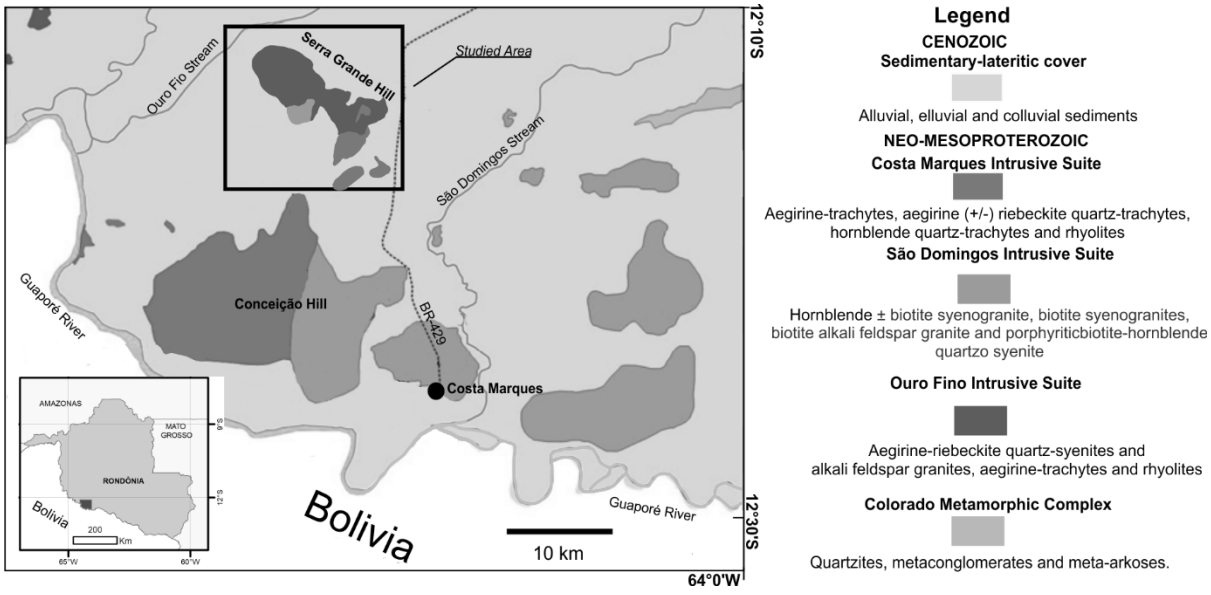

Figure 4.1: Location of the area of study and the vicinal geologyt. Figure extracted from Payolla et al. (2013) and adapted for this work.

It has an alkaline geochemical signature and displays REE enrichments (Freitas et al. 1985). The later characteristic led to detailed research on the Ouro Fino Intrusive Suite through an exploration project with soil and rock sampling conducted by the Geological Survey of Brazil - CPRM (Costa, 1990). The exploration survey executed by the CPRM indicated “frequent geochemical anomalies of Y, La, Zr and Ti” (Costa, 1990). Lately, a study of revaluation of soil samples and airborne geophysical modelling (Buch *et al*., 2018) identified anomalous contents of La, Nd, Yb and Y in the soil and a positive correlation of this anomalies with U and Th detected in aerogeophysical surveys. This study has inferred the Ouro Fino Intrusive Suite as a high potential to become a REE deposit.

In this paper, we present new data about petrography, geochemistry and REE-mineralogy features of the Ouro Fino Intrusive Suite, aiming to advance in the petrological investigation on this new target for REE in the Amazonian craton, Brazil.

4.3. Geological Setting

The State of Rondônia, located on the SW border of the Amazonian Craton, Brazil, hosts several Meso- to Neoproterozoic alkaline (A-type) granitic complexes, representing A-type and within-plate to post-collisional geochemical signatures, which were emplaced during successive magmatic episodes that occurred between 1,606 and 974 Ma (Priem et al., 1971, Isotta et al., 1978, Bettencourt et al., 1999, Quadros and Rizzotto, 2007). Close to the southwest border of the Rondônia State, three A-type granite associations were discriminated in recent studies (Bettencourt *et* al, 2012): Ouro Fino, São Domingos and Costa Marques intrusive suites. The available data place the Colorado Metamorphic Complex as the regional basement (Quadros and Rizzotto, 2007) for those rocks.

4.3.1. Colorado Metamorphic Complex

Colorado Metamorphic Complex is a metasedimentary sequence, formed by metapelitic, metapsammitic, meta-sandstones and meta-arkoses, ferrous-manganesiferous and calcissilicatic rocks (Rizzotto *et* al., 2007). Subordinately occur meta-conglomerates and phyllites (Torres *et* al, 1979; Quadros and Rizzotto, 2007). The Colorado Metamorphic Complex is the supracrustal set of rocks associated with the Alto Guaporé fold belt, an orogeny correlated to the Rondonian-San Ignácio Province (Rizzotto *et* al., 2014; Bettencourt *et* al., 2010).

4.3.2. The Three Alkaline Intrusive Suites

The Costa Marques Complex (Torres et al. 1978) was first named as Costa Marques Granite (Lobato 1966) and later named as Costa Marques Group (Santos et al. 1978). It is composed of porphyritic granites, rhyolites, andesites, tuffs, quartz porphyries, granites and granophyres. According to Bettencourt et al. (2012), the Costa Marques Complex can be divided into three alkaline granitic suites: two plutonic and one subvolcanic. The oldest plutonic suite is composed of aegirine-augite-riebeckite quartz-syenites and alkali feldspar granites. The second plutonic suite is composed hornblende-biotite syenogranites with medium-coarse grained matrix and porphyritic to seriate texture. The subvolcanic suite presents porphyritic hornblende-trachyte and hornblende-rhyolites. These suites were

denominated by Bettencourt et al. (2012) as Ouro Fino Intrusive Suite, São Domingos Intrusive Suites and Costa Marques Intrusive Suite, respectively. From the former Costa Marques Complex, for Costa Marques Intrusive Suite remained only the volcanic lithotypes. Payolla et al. (2013) classified these three igneous suites as an alkali to alkali-calcic, peralkaline to metaluminous, with sodium-potassic affinity. In consonance with these authors, the three igneous suites of Costa Marques feature geochemical characteristics of A-type granites.

The first geochronological data for the former Costa Marques Complex were obtained by Santos et al. (1979), which provided an isochronous of Rb/Sr at the age of 962 ± 72 Ma. With this age, the authors correlated the Costa Marques magmatism to the Rondonia Intrusive Suite magmatism ("Young Granites of Rondônia"). Long after, Bettencourt et al. (2012) obtained new ages by analyzing U/Pb in zircons using the SHRIMP method. The results yield three different ages, permitting to discriminate three magmatic suites in the region. These authors conclude that the Ouro Fino Intrusive Suite is older, with 1347 ± 9 Ma, the São Domingos Intrusive Suite is the subsequent magmatism at the age of 1057 ± 10 Ma and finally, the Costa Marques Intrusive Suite at the age of 998 ± 10 Ma.

Coeval to the Ouro Fino Intrusive Suite magmatism were two other important regional events: the magmatism of the Alto Candeias Intrusive Suite and the metamorphic peak of the Guaporé Fold Belt (Rizzotto *et* al., 2013). The Alto Candeias batholith is a subalkaline suite composed of amphibole-biotite syenogranites, biotite-syenogranites and some charnockites (Bettencourt et al., 1999). According to Bettencourt et al. (1999), U-Pb in zircos yielded ages between 1346 ± 5 and 1309 ± 9 Ma, which are correlated to "an extensional regime related to Rondonian-San Ignacio orogeny or to the opening of the Greenvillian ocean". In the Guaporé Fold Belt, Rizzotto et al., (2013) obtained 207Pb/206Pb ages analysing zircons from a coarse-grained porphyritic monzogranite of the Igarapé Enganado Intrusive Suite. The Concordia age of 1340 ± 5 Ma from this suite is correlated to the peak of metamorphism and deformation in the Guaporé Suture.

4.3.3. Guaporé Formation

Figueiredo et al (1974, in Santos et al., 1978) define as Guaporé Formation the group of sediments, consolidated or not, deposited in the flood plain of the Guaporé River. Torres et al (1978) report intense laterization processes, with lateritic crusts up to 40 meters

in height. Two members were determined to the Guaporé Formation, being the former (inferior) the eluvial-colluvial sediments originated from the erosion of the Serra dos Uopianes hills and the second (superior), the fluvial sediments associated to the present rivers in the region (Torres et al., 1978).

4.4. Methodology

Fieldwork surveys for sampling were performed during the Amazonian summer. For this study, 18 rock samples were analysed. The bulk-rock chemistry was determined by geochemical analyses performed in the laboratory ALS Global using ICP-AES analyses (Service Pack ME-ICP06 – ALS Global, 2018) or major oxides chemistry and ICP-MS (Service Pack ME-MS81 – ALS Global, 2018) analyses for trace and rare earth elements. The samples for ICP-AES assays were prepared on a fused bead with posterior acid digestion. The analytes for the analyses of ICP-MS were prepared using lithium borate fusion and four acid digestion.

The petrographic studies were supported by mineralogical XRD analyses, also developed by ALS Global (Service Pack XRDSQ – ALS Global, 2018).

The samples CM-31 and CM-39 were assayed under the technique X-ray diffraction of rock powder. The analyses were performed by ALS Global laboratory using a Bruker D8 Focus Bragg-Brentano diffractometer with a tube of cobalt. The range of 2θ was between 2º and 70º, with a theta step size of 0.1º and an analysis speed of 1.2 s per step. The mineral composition was determined by the diffractometric results using the Rietveld method. Electronic Microprobe Analyses (EPMA) were performed on six samples, partly at the Federal Institute for Geosciences and Natural Resources (BGR) and at the Laboratory for Microprobe at the Institute for Geosciences of the University of Brasília (LM-IG-UnB). The samples CM-20, CM-28B, CM-31 and CM-39 were analysed by BGR, with given results for Na, Mg, Al, Si, K, Ca, Ti, Mn, Fe, Sr, Y, Zr, La, Ce and Hf. In the (LM-IG-UnB), the samples CM-04 and CM-20 were analysed in three different proceedings: (i) – silicates, aiming to analyse Na, Mg, F, Al, Si, Ca, K, Cl, Ti, Cr, Mn, Sr, Ni, Fe, V and Ba; REE, with results for REE + Na, K, Sr, Pb, Th, U and Ba; (ii) – major elements, with results for F, Al, Si, Hf, Nb, P, Ti, Mn, Y, Ta, Ca, Zr and Fe and (iii) – REE, with results for REE + Na, K, Sr, Pb, Th, U and Ba. The two former analysis stages were performed to determine the mineral, being the first for silicate minerals (e.g. arfvedsonite) and the second on potential hosts for REE (e.g. zircon). The third proceeding was performed to determine REE content in the analysed

minerals. The analytical parameters used for the EPMA analyses are in the Appendix I. The geological map presented in this work (Fig. 2) was supported by fieldwork data integrated with geophysical data from Buch *et al*. (2018) and CPRM (2010).

4.5. Field and Petrographic Aspects

The area of study comprises the locally known Serra Grande hill and its vicinities. The Serra Grande hill is a very pronounced elevation on the Guaporé flood plain, 25 km NNW of the city of Costa Marques, elongated in NW-SE direction, 10 km in length and 2 km wide. Around the hill, there is a wide plain with little morphological changes.

The Serra Grande hill represents mainly the outcrop of the Ouro Fino Intrusive Suite and during this study, it was discovered that the São Domingos and Costa Marques intrusive suites also outcrop in the area (Fig. 4.2). Around the Serra Grande Hill, there are lateritic crusts and the clastic deposits from the Guaporé Formation. Locally also alluvial and colluvial clastic deposits occur which are related to the current depositional dynamic environment.

4.5.1. Ouro Fino Intrusive Suite

The Ouro Fino Intrusive Suite is a massive stock domaining the area of the Serra Grande Hill. Other small plutons in the NW of Costa Marques also occur in the same directional trend (Fig 4.1). The Ouro Fino Intrusive Suite is covered by scattered vegetation and is covered on its borders by laterites (Fig 4.3.a). The outcrops are usually big exposure of rocks, though, given the tropical climate, the rocks present variable degrees of weathering (Fig 4.3.b).

Bettencourt et al. (2012) define the Ouro Fino Intrusive Suite as aegirine-augite-riebeckite quartz syenites and alkali feldspar granites. In this study, these lithotypes are found in almost all the Serra Grande Hill, and the granite subfacies are differentiated mainly by texture. In mesoscopic scale, the granitoids are gray to pinkish gray, with a phaneritic seriate to the equigranular texture that varies from fine-middle grained (fmg subfacies) up to coarse-middle grained (cmg subfacies) and a massive structure.

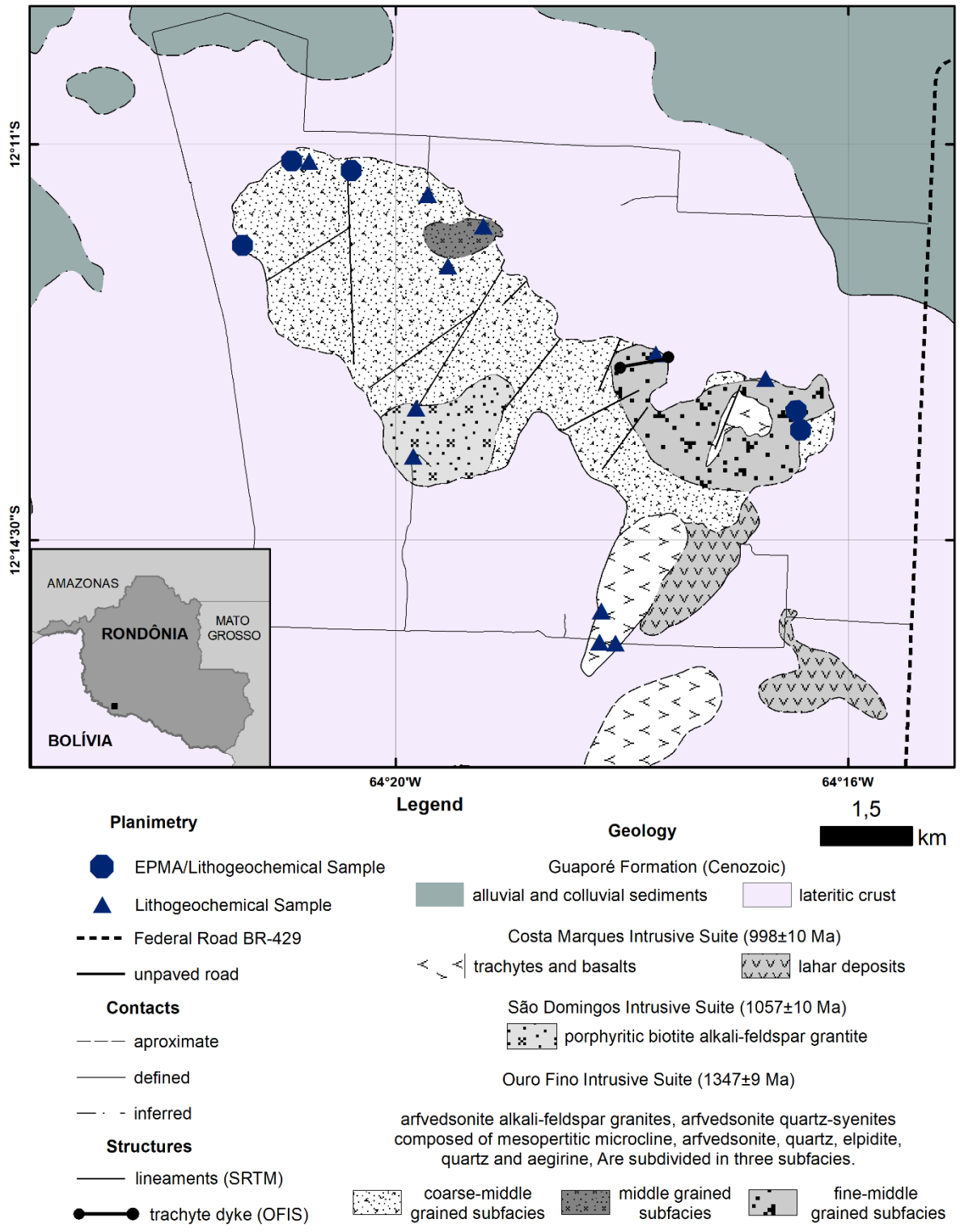

Figure 4.2: Geological map of the studied area and location of the studied samples.

The cmg subfacies is the dominant variety of alkali feldspar granites and quartz syenites (Fig. 4.4.a). The rock is composed by subhedral microcline, euhedral to subhedral elongated crystals of Na-amphibole and interstitial anhedral quartz. In this subfacies, the

microcline tends to be more euhedric and the amphibole crystals are larger compared with microcline and amphiboles of the other subfacies.

The fmg subfacies occurs in a very restricted region, in the central part of the ridge (Fig 4.2). It is mainly composed of a grey-pinkish equigranular matrix of subhedral to euhedral alkaline feldspar, subhedral sodic amphiboles and interstitial anhedric quartz (Fig 4.4.b).

In the eastern portion of the hill outcrops the medium equigranular subfacies (mg) with a greenish-grey matrix composed of subhedral to anhedaal microcline, subhedral ripiform sodic amphiboles and anhedral quartz (Fig 4.4.c).

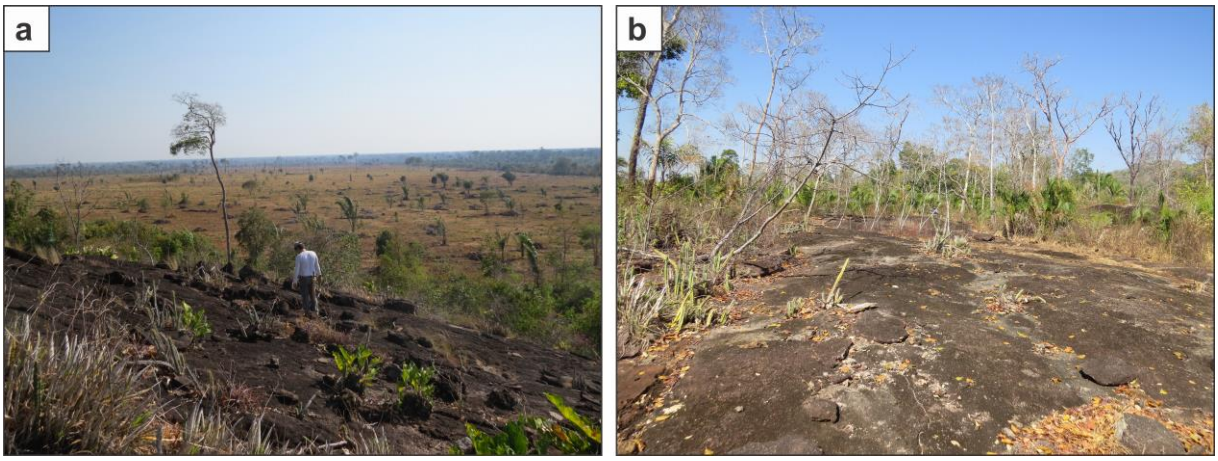

Figure 4.3: a – The Ouro Fino Intrusive Suite is surrounded by the Guaporé River floodplain; b – Outcrop in the Serra Grande Hill. The vegetation is scarce, giving a good rock exposure.

In the eastern portion of the area, the syenite is intruded by a a decameter-wide trachytic dyke. The trachyte represents volcanic facies of the Ouro Fino Intrusive Suite. It has an aphanitic matrix and phenocrystals of alkaline feldspar and sodic amphiboles (Fig. 4.4.d). Enclaves are found in the northwest area associated with the cmg subfacies. Part of these enclaves is round shaped xenoliths with an aphanitic gray matrix and ripiform phenocrystals of feldspar (Fig. 4.4.e). Also, pegmatoid pods are sparsely found associated with cmg subfacies, where centimeter-sized euhedral amphibole and centimeter-sized anhedral quartz are found.

Another feature is the clusters of Na-amphibole indicating local magmatic flow (Fig. 4.4. f). Also, a very important feature of these granites is the presence of interstitial fine grained elpidite (Fig 4.4.a, b, c). The elpidite is the mineral that gives to the Ouro Fino Intrusive Suite a pink coloured aspect and reaches up to 5% of the modal mineralogy. Small

scale elongated quartz veins crosscut the granite stock and are parallel to the main NW-trend.

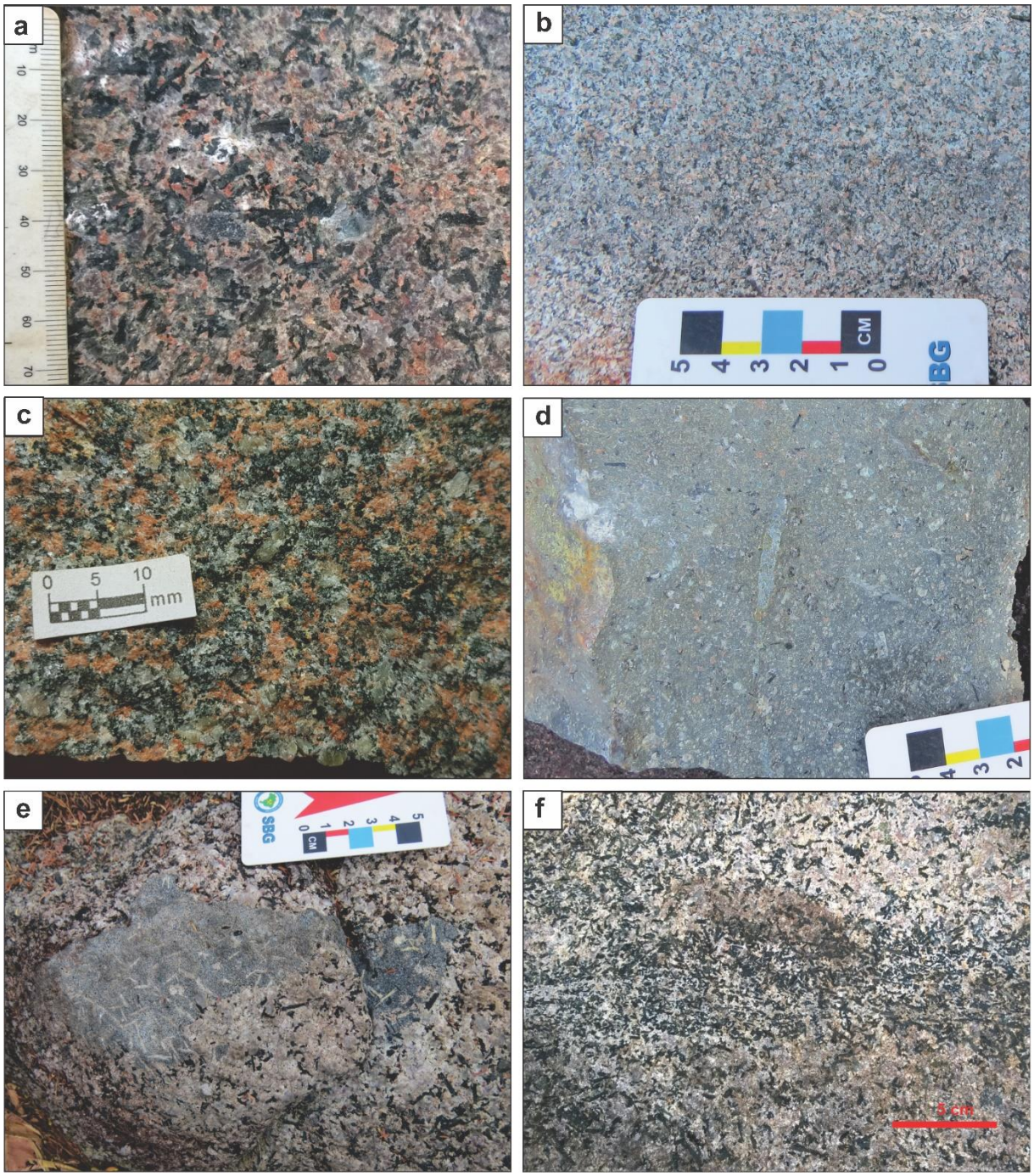

Figure 4.4: a – coarse-midle grained subfcacies exhibiting a phaneritic equigranular texture; b – fine-middle grained subfaces with pervasive presence of elpidite in the rock matrix; c – middle grained subfacies of the Ouro Fino Intrusive Suite; d – trachyte dyke with scattered phenocrystals of Na-amphibole and K-feldspar and aphanitic grey matrix ; e – Enclave with mafic aphanitic matrix and ripiform K-feldspar phenocrystals; f – Local magmatic flow of Na-amphiboles.

In microscopic scale, differences in grain size are less evident on the microscopic scale. The variable grain size of microcline causes granulometric differences between the subfacies. The rocks of the Ouro Fino Intrusive Suite are holocrystalline, leucocratic, medium grained and equigranular to seriate texture (Fig 4.5.a, b). The main minerals observed in thin section are micropertitic microcline, arfvedsonite rimmed by aegirine, quartz and elpidite (Fig. 4.5.c, d). Titanite, zircon, analcime, garnet and aenigmatite occur subordinately in sub- to anhedral, fine-grained habits. (Fig. 4.5. e, f).

The microcline exhibits euhedral to subhedral crystals with compositional zoning and micropertitic exsolution. The crystals usually are squared and are often seen as inclusions inside of the Na-amphiboles. Also, some crystals present very fine-grained inclusions that resemble zircon and apatite. In some samples, the microcline presents subtle albitization, with fine grained anhedral albite. The main Na-amphibole is arfvedsonite, occurring as subhedral to euhedral ripiform crystals. Its edges are frequently rimmed by aegirine and the replacement in some crystals is quite intense, being the aegirine overplacing the arfvedsonite.

Quartz is medium- to fine-grained and occupies interstices between the other minerals. The form of the crystals is defined by the shape of the surroundings crystals and the contacts are usually curvy to straight. Some inclusions of euhedral microcline crystals are scattered in the quartz crystals. Undulatory extinction is a common feature in these crystals. The elpidite occurs in clusters of fine to very fine-grained crystals associated with fine-grained anhedral quartz and with anhedral zircon. The zircon is always anhedral, yellow coloured and fine grained. It is always occupying voids and interstices between the the major minerals. Along with zircon, the titanite fills the interstices of the rock. Analcime, garnet and aenigmatite are rare and if present, they are anhedral and fine-grained. The table 1 (Appendix 1) summarizes the modal mineralogy from the Ouro Fino Intrusive Suite that had been identified in the petrographic studies.

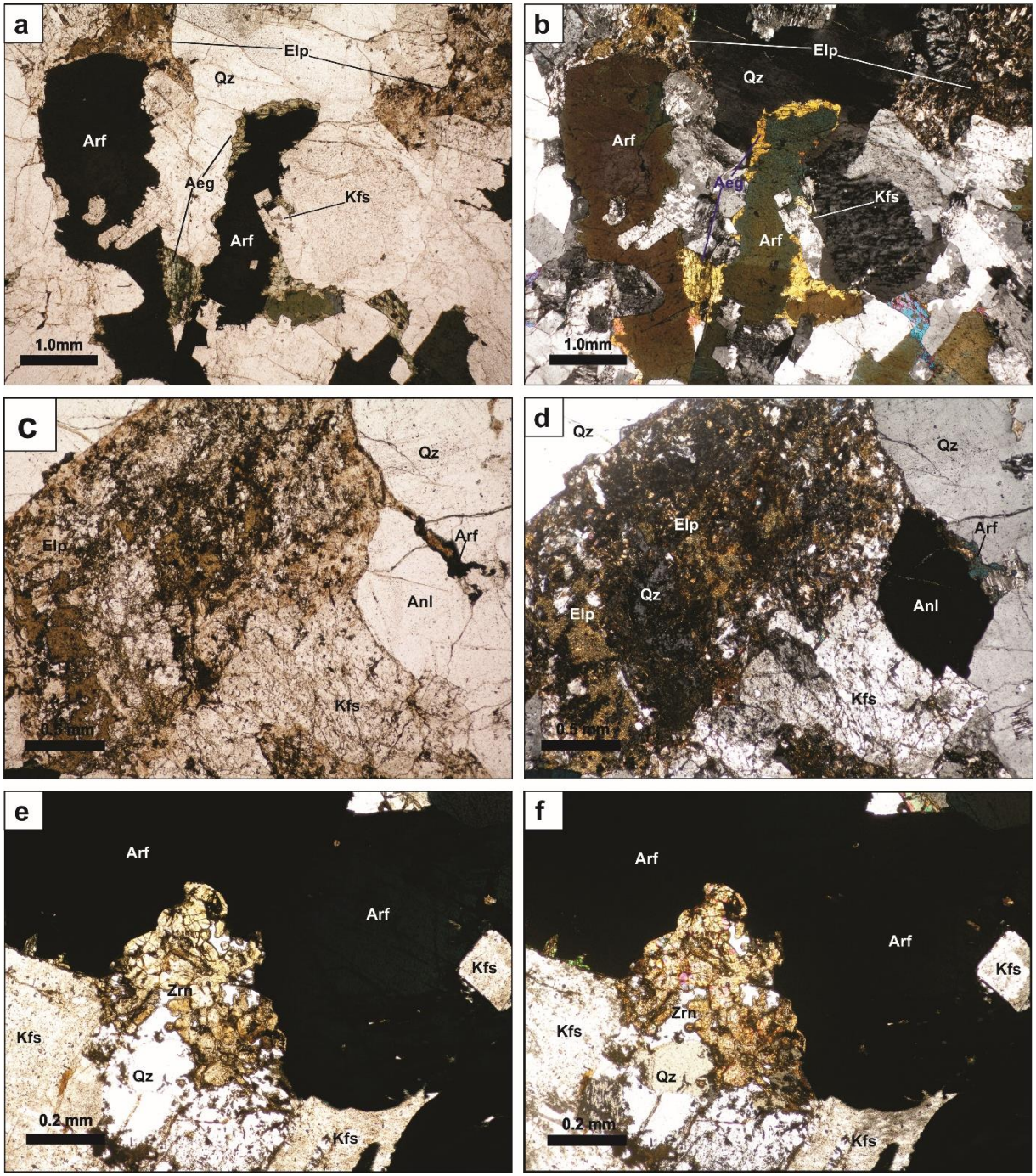

Figure 4.5: Transmitted light micrographs of thin sections with parallel (left) and crossed nicols (right). a and b – General texture of the cmg subfaces. Note the arfvedsonite crystals rimmed by aegirine; c and d – cryptocrystalline elpidite crystals associated to quartz inside primary elpidite pseudomorphs; zircon crystals occupying interstices between the major minerals; e and f – crystals of zircon filling voids between the major minerals. Mineral abbreviation: Aeg – Aegirine; Anl – Analcime; Arf – Arfvedsonite; Kfs – Potassic Feldspar; Elp – Elpidite; Qz – Quartz; Zrn – Zircon.

The modal mineralogy from the cmg and fmg subfacies was also verified through XRD analyses using the Rietveld method to interpret the mineralogical composition. The

mineralogical results from the XRD of rock powder analyses are displayed in Table 2 (Appendix 1). The two analysed samples represent the two most common phases of the Ouro Fino Intrusive Suite Suite, the fmg and cmg phases. The results display relative equal contents of sodic and potassic feldspars, evidencing thus the hypersolvus character of the massif. The quartz exhibits higher content than expected from the optical estimation of the thin sections. The results for mafic minerals suggests that in the cmg granites. there is less aegirine than in the fmg lithotype. Elpidite, which composes between 5 and 10 % of modal mineralogy was not identified in the DRX assays.

4.5.2. São Domingos Intrusive Suite

The southern-central part of the massif presents a pink grayish granitoid, with a porphyritic texture defined by pink K-feldspar crystals in a fine grained equigranular matrix composed of amphibole, K-feldspar and quartz. This porphyritic granite is part of the São Domingos Intrusive Suite. The phenocrystals are euhedral to subhedral and dominate the matrix (80% of K-feldspar). The amphiboles are needle-shaped and the quartz, subordinately occupy the interstices between the other crystals. Like the Ouro Fino Intrusive Suite, the São Domingos Intrusive Suite presents enclaves that have a brecciated appearance, with angular forms and vary from a very hololeucocratic matrix defined by alkaline feldspar to a melanocratic aphanitic mafic composition matrix composed of fine-grained mafic minerals.

Microscopically, these granitoids display a seriate texture. The microcline presents intense micropertitic intergrowth. Plagioclase is fine to middle grained, tabular shaped and subhedral form and can substitute microcline in the rims. Quartz is anhedral to subhedral and is interstitial between other minerals. As mafic minerals, there is subhedral medium-grained biotite. Opaque minerals occur scattered throughout the rock. Whereas in the Ouro Fino Intrusive Suite the euhedral zircon is absent, the São Domingos Intrusive Suite shows zircon crystals with euhedral form.

4.5.3. Costa Marques Intrusive Suite

The eastern part of the Serra Grande hill is intersected by a diabase/dacite dyke, of N10E trend. The rock has a porphyritic texture defined by milimetric euhedral crystals of K-feldspar and a gray aphanitic matrix. Veinlets of anhedrical fine grained K-feldspar cut the

rock. Millimeter-sized amygdalae occur frequently in the rocks. Southwards from the Serra Grande, there are volcanic breccias associated with trachytes.

4.6. Geochemistry

The geochemical results are from 18 rock samples and permitted not only to classify the rocks but also to discriminate the volcanic rocks of the Ouro Fino Intrusive Suite from the Costa Marques Intrusive Suite and São Domingos Intrusive Suite, which occurrence in the Serra Grande Hill was up to date unknown. Among the 18 analysed rocks, 13 are from the Ouro Fino Intrusive Suite, 2 from the São Domingos Intrusive Suite and 3 from the Costa Marques Intrusive Suite. All the three subfacies of the Ouro Fino Intrusive Suite were analyzed along with a trachyte dyke. The basalt that is part of to the Costa Marques Intrusive Suite is not included in the charts of Fig 4.9 once these diagrams are not suitable for this kind of rock. Some samples of the Ouro Fino Intrusive Suite yielded Zr content more than the upper detection limit (10,000 ppm) and thus, these Zr contents are considerate as 10,000 ppm in order to permit the plots. The geochemical results for the three suites are exposed in Table 3 (Appendix 1).

In accord with Frost *et* al. (2001), the figure 4.6.a shows the $FeO^{tot}/(FeO^{tot}+MgO)$ plots for the Ouro Fino Intrusive Suite, São Domingos Intrusive Suite and Costa Marques Intrusive Suite. In this chart, all the three suites display a strict ferroan character. However, in the MALIxSiO_2 plot (Frost *et al*. 2001), the Ouro Fino Intrusive Suite presents a variation between alkaline and calc-alkaline (Fig. 4.6.b). The calc-alkaline types are the trachyte dyke, fmg, mg and cmg subfacies, whereas the cmg and mg subfacies show higher variability. The São Domingos Intrusive Suite and Costa Marques Intrusive Suite plot only in the alkaline field.

Consonant with Maniar and Piccoli (1989), the Ouro Fino Intrusive Suite features a peralkaline pattern in the chart A/NK x A/CNK chart (Fig. 4.6.c). Moreover, the São Domingos Intrusive Suite exhibits a peralkaline composition whereas the Costa Marques Intrusive Suite is metaluminous. In the three charts (Fig. 4.6 d, e, f) for discrimination between A-type and I- or S-type granites, the Ouro Fino Intrusive Suite presents a distinct A-type granite character (Whalen *et* al., 1987). The São Domingos Intrusive Suite and Costa Marques Intrusive Suite are also included in the A-type field, but litte less prounounced. The

Zr, Ce and Y contents of the Ouro Fino Intrusive Suite are 10-times higher compared to the Costa Marques Intrusive Suite.

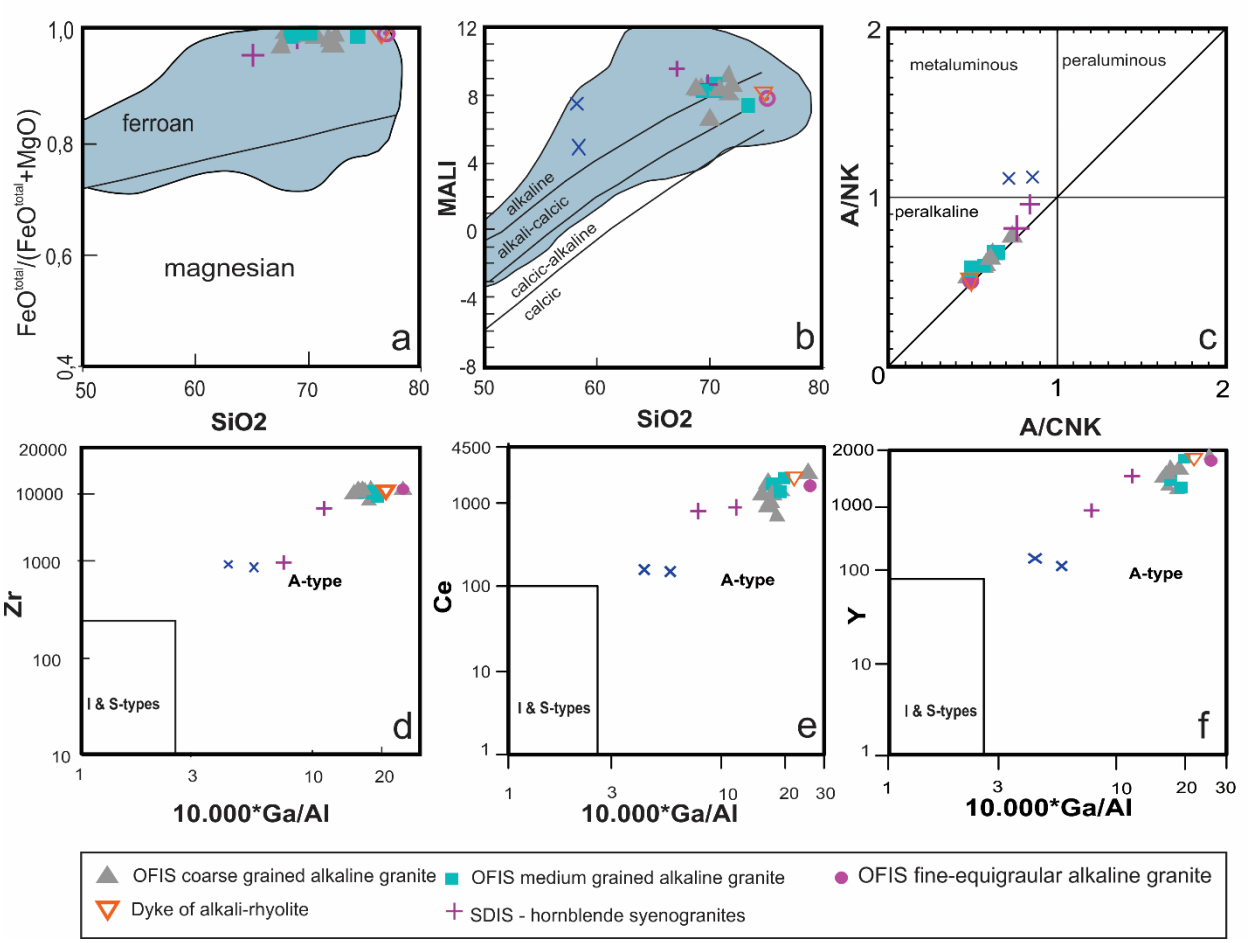

Figure 4.6: Binary diagrams of the chemical results from the silica saturated rocks of the Ouro Fino Intrusive Suite (OFIS), São Domingos Intrusive Suite (SDIS) and Costa Marques Intrusive Suite (CMIS) in accord to Frost et al. (2011) – a and b; Maniar and Piccoli (1989) - c; Whalen et al. (1987) – d, e and f.

The REE contents normalized to the chondrite of Boynton (1984) show clear discrepancies between the Ouro Fino Intrusive Suite and Costa Marques Intrusive Suite, though not so evident discrepancies between the São Domingos Intrusive Suite and Ouro Fino Intrusive Suite (Fig. 4.7). In the Costa Marques Intrusive Suite, the REE-patterns display a discrete Eu anomaly and also a flat line in the basalt sample. In the Costa Marques Intrusive Suite, the LREE are slightly enriched compared to HREE, yielding an average $(La/Yb)_n = 5.15$.

The Ouro Fino Intrusive Suite reveals different enrichments for LREE in relation to HREE (Fig. 4.7). The average $(La/Yb)_n$ rate for the cmg subfaces is 7.36 and for the fine-

middle grained 10.42. The only sample of the middle grained subfaces shows (La/Yb)n = 6.92. The São Domingos Intrusive Suite evidence $(La/Yb)_n$ rates of 12.49 – similar to the fmg of the Ouro Fino Intrusive Suite.

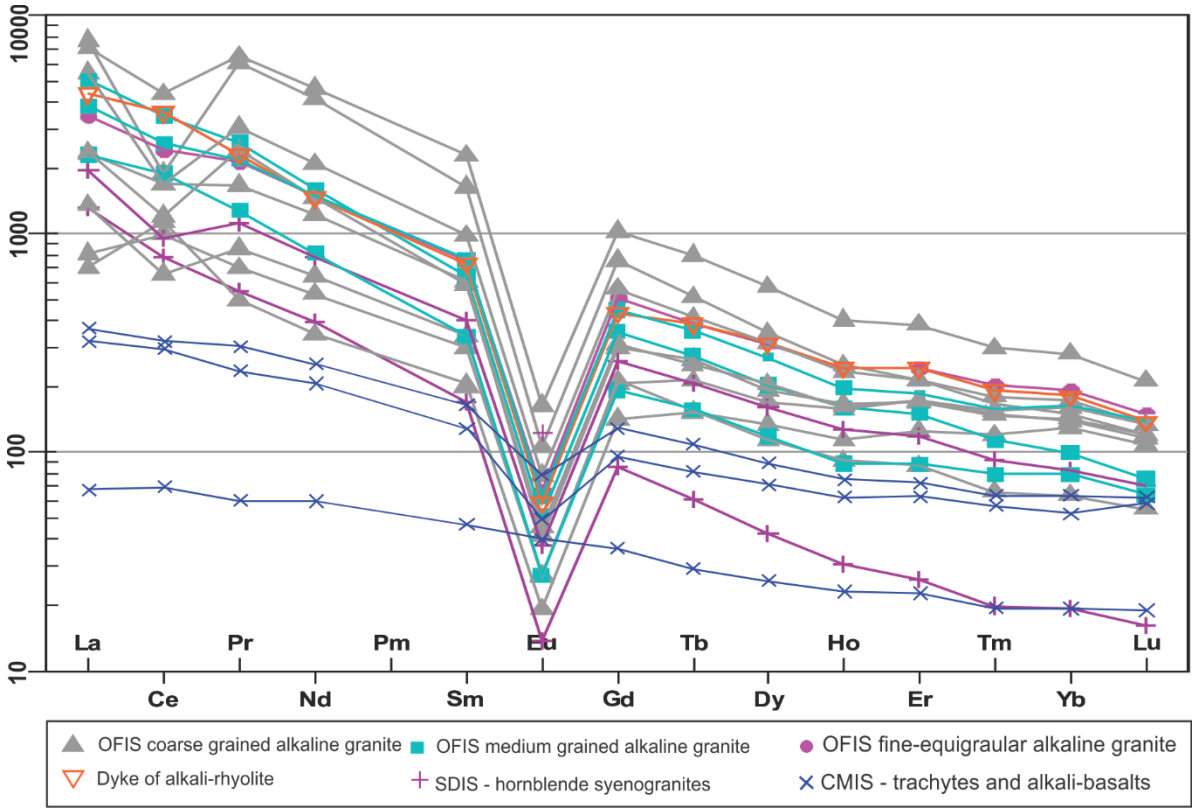

Figure 4.7: REE content of the analysed rocks from the Costa Marques (CMIS), São Domingos (SDIS) and Ouro Fino (OFIS) intrusive suites normalized to the chondrite of Boyton (1984).

Europium anomalies are distinct in both Ouro Fino Intrusive Suite and São Domingos Intrusive Suite. In accord with the figure 4.7, some samples of the Ouro Fino Intrusive Suite displayed Ce anomalies, either with some Ce depletion or enrichment.

The Fig. 4.8 presents the multielement chart with the chemical results from the three suites after normalization to the chondrite of Thompson (1982). The Costa Marques Intrusive Suite presents K enrichment whereas the Ouro Fino Intrusive Suite and São Domingos Intrusive Suite are depleted in this element. Strontium, P and Ti form negative anomalies in the Ouro Fino and São Domingos intrusive suites, however, in the Costa Marques Intrusive Suite, these elements are slightly depleted. The lower contents of Ba and higher contents of Zr, Hf, Y and REE permit a clear distinction between the of the Ouro Fino Intrusive Suite

and the other two suites, resulting thus in the geochemical discrimination of the rocks that outcrop in the Serra Grande Hill. The higher contents of Zr, Hf, Y and REE can be related to the zircon and elpidite (zirconosilicates) that are absent in the Costa Marques Intrusive Suite and less frequent in the São Domingos Intrusive Suite, in which only primary zircon has been identified.

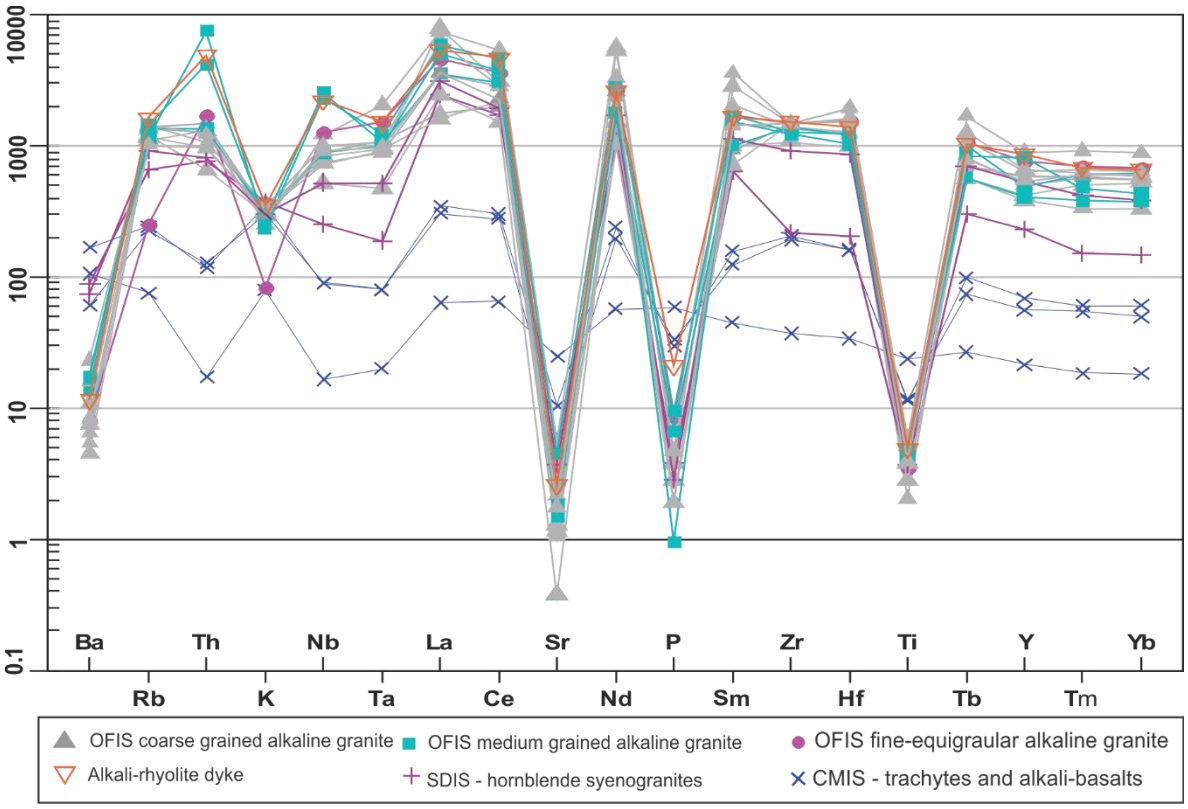

Figure 4.8: Chemical results chart from the analysed samples from the Costa Marques (CMIS), São Domingos (SDIS) and Ouro Fino (OFIS) intrusive suites normalized to the chondrite of Thompson (1982).

In accord with Eby (1992), the Ouro Fino Intrusive Suite and São Domingos Intrusive Suite fit into the A2-type granite (Fig. 4.9.a, b). Although, one sample presented an A1-type pattern, what could be considered as possible hydrothermal alteration.

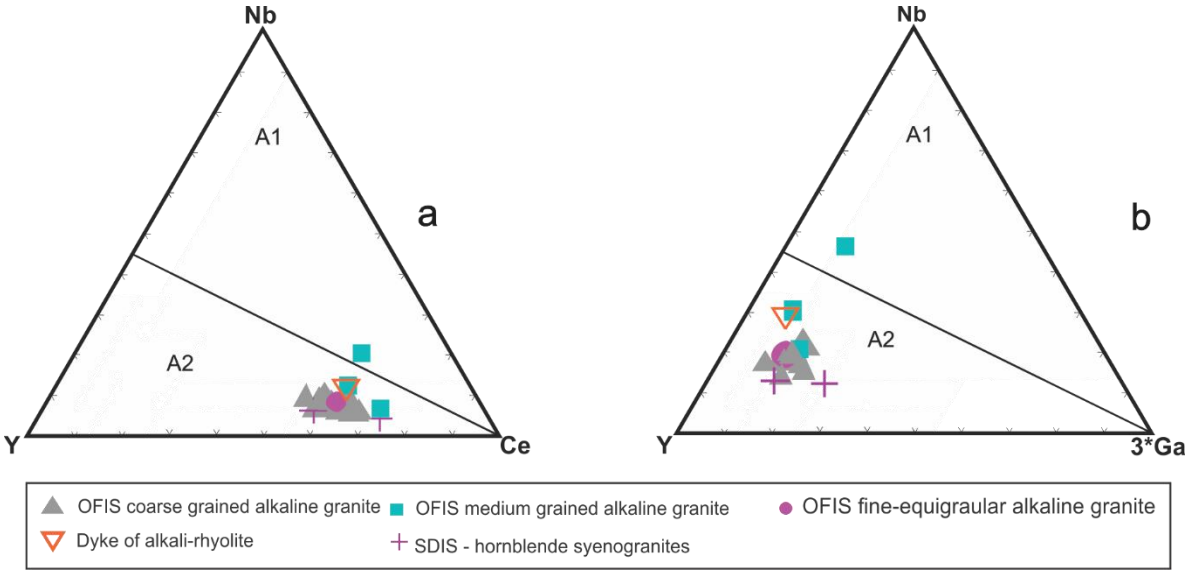

Figure 4.9 Classification of alkaline granites in accord with Eby (1992) for the rocks of the São Domingos and Ouro Fino intrusive suites. a – ternary diagram Y-Nb-Ce; b – ternary diagram for Y-Nb-3*Ga.

4.7. Mineral Chemistry

Electron probe microanalyses (EPMA) were performed on 6 samples from the Ouro Fino Intrusive Suite. Among, these 6 samples, the samples CM-20B, CM28C, CM31 and CM39 were analysed at BGR in Hanover, Germany. The samples CM18 and CM20A were analysed in the EPMA laboratory from the Universidade de Brasília. All the samples are alkali feldspar granites with sodic amphiboles, 5 from the cmg subfacies and one from the fmg subfaces (CM31). The targeted minerals were amphiboles, aegirines rimming the amphiboles, titanite and the zirconosilicates (elpidite and zircon). The classification of amphiboles was made in accord with the spreadsheet of Locock (2014), the pyroxenes were defined with the aid of the software PX-NOM (Sturm, 2002).

The main amphibole identified in the EPMA analysis is arfvedsonite (Table 4). In accord with the classification of Locock (2014), the mineral chemistry leaded to the identification of ferro-eckermannite and fluor-arfvedsonite. However, the chemical composition of the analysed amphiboles did not differ significantly, therefore the single term arfvedsonite is more appropriate for this work. The analysed pyroxenes were always at the rims of the Na-amphiboles. In accord with the PX-NOM software, all the pyroxenes are strictly aegirine. Compared to the aegirine, arfvedsonite presents a higher CaO budget. Moreover, the arfvedsonite exhibits F contents yielding between 1.44% and 2% of F.

Titanite, zircon and elpidite were defined in accord with the stoichiometric balance for the calculated oxides of the analysed elements. Moreover, for the zirconosilicates, a classification scheme created by Salvi and Williams-Jones (1995) was used given the relationship between these minerals with mineralization (Fig. 4.12). The mineral chemistry results and classification of the analysed amphiboles and pyroxenes are shown in table 2. The mineral chemistry results for analysed zircon and titanite are in table 5 and for elpidite in table 6.

In accord with the EPMA results (Fig 10.a, b), the zircon yields TREO+Y (total rare earth oxides + yittrium oxide) values from 3.2% up to 7.3% (Table 5). The titanite also contains REE+Y in its structure, but the TREO+Y content ranges in a lower interval between 1.07 and 3.53% (Table 5). Analyses of elpidite (Fig 10.c, d) show Y2O3 contents ranging from 0.21 up to 1.92 wt.%, but low LREE (La, Ca) contents (Tab 4). An enrichment of CaO was observed in the elpidite, hence defining the elpidites of the Ouro Fino Intrusive Suite as Ca-elpidite given the trend towards gittinsite and armostrongite (Fig 4.12). The CaO contents vary from 0.30 in elpidites from the cmg subfacies (CM-39) up to 3.01% in the fmg subfacies (CM-31), with an average of 1.75%. K_2O contents are also high in some elpidite crystals, ranging between 4.18% and 6.94% whereas when in low content, ranges between 0.26 and 0.65%.

The zircon and the elpidite can be considered important hosts for Zr and Hf. The Zr and Hf in the zircon vary from 56.17% up to 59.87% and 0.93% up to 1.49%, respectively (Table. 5). Elpidite carries less Zr and Hf amounts with values ranging from 18.9% up to 21.82 % for Zr and for Hf the variability lies between 0.34% up to 0.57% (Table 6). Nonetheless, elpidite content in the Ouro Fino Intrusive Suite reaches up to 5% in a modal estimative. becoming the major REE-Zr host in the Ouro Fino Intrusive Suite. The titanite presents some enrichment of Y, La and Ce reaching around 3% in total (Table 5.).

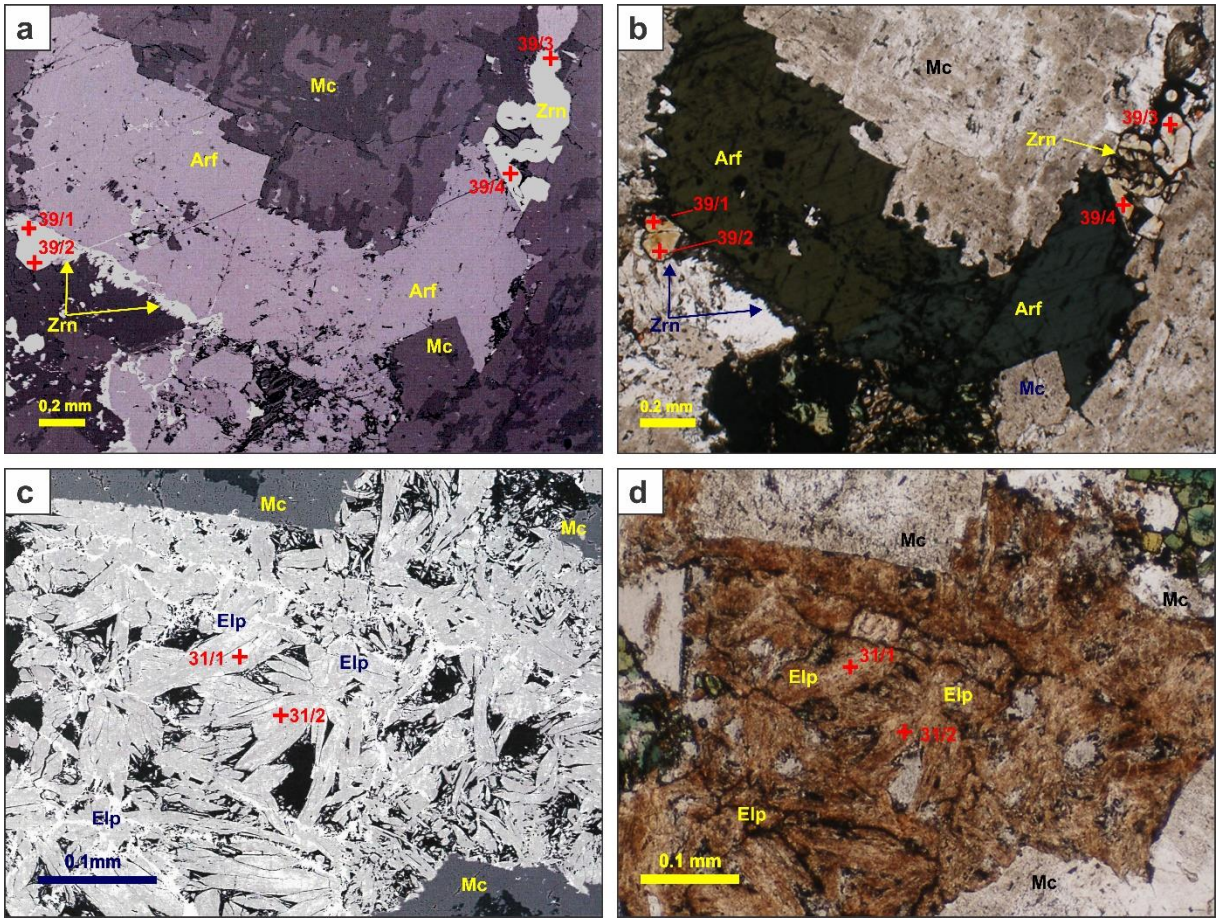

Figure 4.10: a – zircon occupying void beside arfvedsonite crystal. BSE image; b – Same detail from the previous image, now in under the plane polarized light; c – elpidite crystals cluster and the spots where the crystals were analysed by EPMA. BSE image; d – The same elpidite cluster seen under the plane polarized light.

Since zircon is the mineral that contains the highest content of REE+Y in the Ouro Fino Intrusive Suite, WDS analyses targeted a zircon from the sample CM18. The Fig. 4.11.a shows the analysed minerals, and Table 7 exhibits the respective chemical WDS analyses from the spots 31/1, 31/2 and 31/3. The spot 31/2 target the centre of the crystal and spots 31/1 and 31/2 analysed the surrounding area. The zircon yielded TREO+Y of 5,15%, however, the surrounding area of the analysed crystal presented 16.83% and 23.83% of TREO+Y for the spots 31/1 and 31/3 respectively (Table 7). Though, the targeted area of spots 31/3 did not fill the stoichiometric composition of zircon, being not possible to determine which mineral the crystal needles might represent. The spot 31/1 represents the chemical composition of the mass rimming these acicular minerals and the zircon (Fig 4.11.b). The rimming mass is composed mainly of SiO (27.4%). FeO (14.6%). CaO (10.9%) and ZrO (7.2%), being also not possible to determine which mineral it could represent. In

the needle around the zircon boundary, REE occur mainly as La2O3 (5.9%), Ce2O3(8.1%), Nd2O3(1.1%). The other REE occur variable and less significative amounts. For the mass rimming the zircon and the acicular crystals, Ce is the dominant REE. In both spots 31/1 and 31/3, F was not detected.

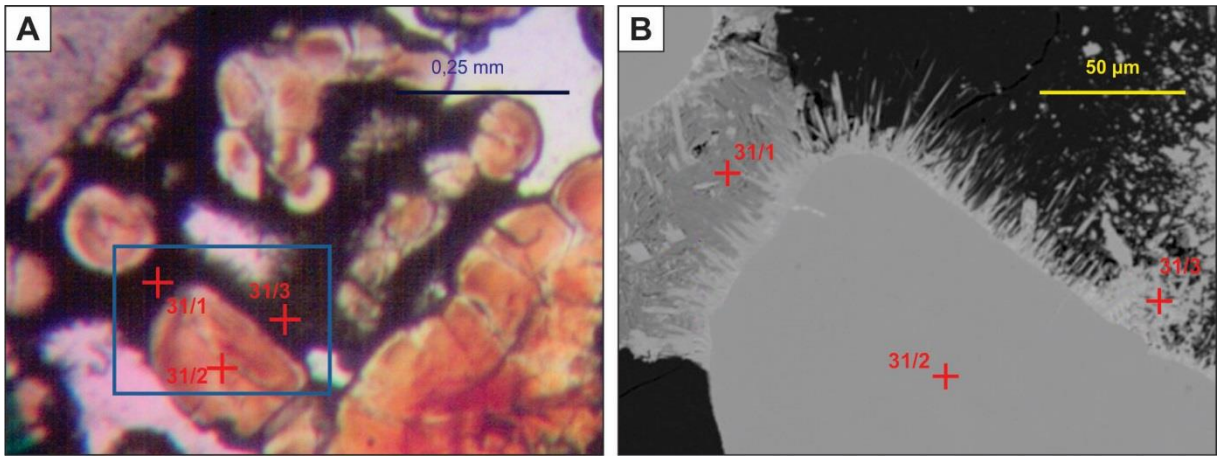

Figure 4.11: a – Detail of zircon assayed with WDS and EDS analyses; b – The SEM image is the detailed region inside the blue square. Note the mass and needles grown on the zircon crystal boundary.

4.8. The Origin of the REE-Zr Mineralization

The new mapping for the region of Serra Grande Hill (Fig. 4.2) shows two other igneous units outcropping in the area. Despite the fact that the Costa Marques and São Domingos intrusive suites are also alkaline (Payolla et al., 2013, this work), the petrographic features associated with geochemical data and previous surveys (Costa, 1990; Buch et al., 2018) demonstrate that the REE-Zr mineralization is constricted to the Ouro Fino Intrusive Suite.

According to with Eby (1992), the Fig. 4.9 shows that the Ouro Fino Intrusive Suite and the São Domingos Intrusive Suite originated from the melting of continental crust. Bettencourt et al. (2014) state that isotopes of Hf confirm the old crustal source for the magmas of the Ouro Fino Intrusive Suite whereas the São Domingos Intrusive Suite is of juvenile and crustal origins. The REE chart indicates that the fractionation of LREE in the São Domingos Intrusive Suite is greater than in the Ouro Fino Intrusive Suite, even though the fmg subfacies show similar values (Fig. 4.8).

The absence of primary magmatic zircon and the outstanding elpidite content of the Ouro Fino Intrusive Suite compared to the São Domingos Intrusive Suite endorse the assertion that the Ouro Fino Intrusive Suite is the host of the REE-Zr mineralization.

4.9. Comparison with Similar REE-Zr Deposits

The chemical, petrographic and mineralogical results of this study point out the existence of a REE-Zr mineralization in the Ouro Fino Intrusive. Rare metal mineralizations are related to alkaline granites such as Strange Lake, Kahn Bogd and Kaldzan-Buregtey (Salvi and Williams-Jones. 1990; Gysi and Williams-Jones. 2013; Kovalenko *et* al.. 1995; Kynicky *et* al.. 2011). In these deposits, the main ore minerals are sodic-calcic zirconosilicates like elpidite, armstrongite, gittingsite, catapleiite, zircon and eudialyte.

In the Strange Lake deposit, the mineralization is related to elpidite crystallized under magmatic conditions, whereas the Ca-zirconosilicates (armstrongite and gittinsite) are the result of late stage metasomatic processes, thus replacing primary elpidite (Salvi and Williams-Jones. 1995). In Khan-Bogd and Strange Lake, there is a lack of primary zircon and magmatic elpidite is abundant (Kynicky *et* al., 2011; Salvi and Williams-Jones, 1995). As well, the replacement of elpidite for Ca-elpidite and armstrongite happens in Khan-Bogd. The results of our study indicate that these characteristics appear likewise in the Ouro Fino Intrusive Suite.

In the Ouro Fino Intrusive Suite, the Ca-Zr silicates are absently reflecting the low content of Ca_2^+ in the fluid. Though the fig. 4.12 shows that elpidite and zircon present a trend towards gittinsite and armostrongite. being the elpidite from the cmg subfaces the most calcic. The blurry aspect of the elpidite in thin-section and SEM images support the hypothesis of secondary origin. The enrichment of K_2O in elpidite is still not well understood, however, the elpidites of Khan Bogd present K_2O enrichments as well (Grigor'eva et al., 2011).

The lack of gittinsite in the rock could be related to the absence or insufficiency of Ca^{2+} in the fluid. Additionally, titanite could be a Ca^{2+} consumer during the metasomatic processes. The Ca could be originated from the amphiboles structures since the amphiboles presented up to 6% of CaO in the mineral chemistry results (Table 4).

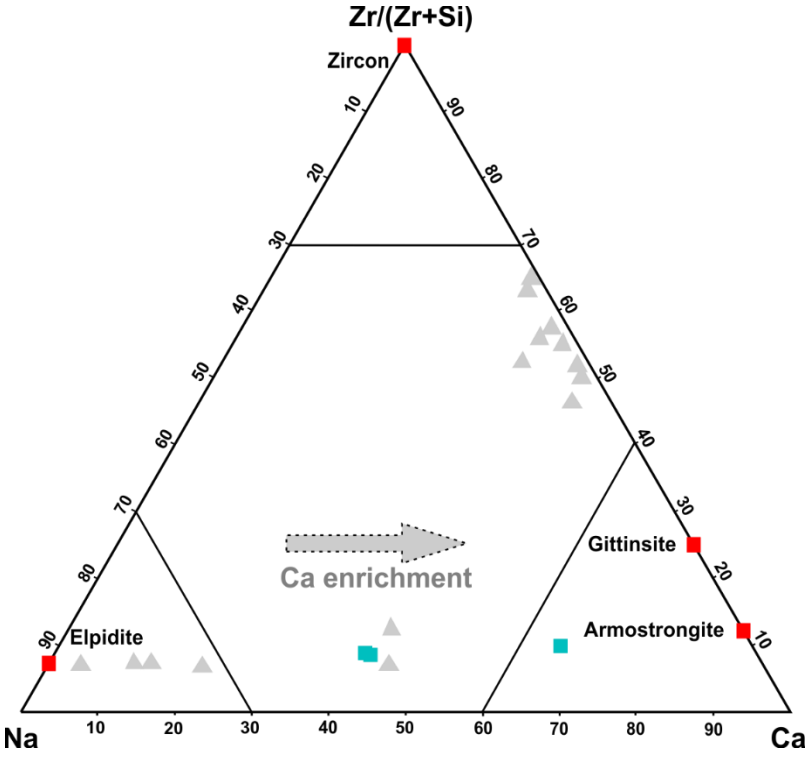

Figure 4.12: Ternary diagram for Na, Zr and Ca in cation proportion for the zirconosilicates of the Ouro Fino Intrusive Suite. The grey triangles indicate zirconosilicates from the cmg subfaces and the blue squares from the fmg subfaces. The red squares represent the respective end-members compositions. Diagram adapted from Salvi and Williams-Jones (1995) and Gysi et al. (2016).

4.10. A Mineralization Model for the Ouro Fino Intrusive Suite

In this work, no other other minerals that might contain REE in the Ouro Fino Intrusive Suite have been identified. The occurrence of xenotime and bastnaesite, which are common in other deposits (Gysi and Williams-Jones, 2013; Michael *et* al, 2017; Chakhmouradian and Zaitsev, 2012), are reported in previous works (Freitas, 1985; Costa, 1990; Costa, 1988) whereas in this work, the presence of these minerals is still not confirmed. Moreover, this study does not comprise F analyses in the bulk-rock chemistry, but the mineral chemistry analyses for arfvedsonite and aegirine evidence a depletion of F from the arfvedsonite during transformation to aegirine (table 2), suggesting F as an active agent during the ore formation processes. In addition, the zircon crystals and the mass around them yielded none F content, what could imply a release of F from Na-amphiboles before the mineralization. Another possibility is the fractionation of F in the lattice of Ca-elpidite, resulting in the capture of F from the fluid before the crystallisation of zircon. These

hypotheses suggest the hydrothermal-deuteric mineralization happened without or little amount F in the system and explains the lack of REE fluoride minerals in the Ouro Fino Intrusive Suite.

In fact, the absence of F in the mineralization fluid is not impeditive to transport REE but to precipitate them (Migdisov *et* al., 2016). These authors define S and Cl as main ligands for transport of the REE at hydrothermal conditions, whereas the presence of F reduces the stabilities of REE in hydrothermal fluids. Indeed, the elpidite concentrations up to 5% in the rock matrix place this mineral as the main ore mineral for the Ouro Fino Intrusive Suite mineralization.

The significant amount of Ca-elpidite, or pseudomorphs of elpidite, suggests H_2O dominated crystallization conditions and classify the Ouro Fino Intrusive Suite as agpaitic despite the fact that the hydrothermalism resulted also in zircon, which is considered a mineral of miaskitic rocks (Marks and Markl, 2017). The deposition of REE, in this case, could be associated with the inclusion into the structure of the zirconosilicates, which are REE-free minerals. Migdisov *et* al. (2016) consider that the incorporation of REE into the lattice of non-REE minerals is one of the effective fractionation mechanism for REE.

The needles and the mass rimming zircon crystals exhibit SiO_2, FeO, CaO and ZrO contentss associated with high concentrations of La_2O_3, Ce_2O_3 and Nd_2O_3. The mass and the needles might have precipitated onto the edges of zircon during the decrease of hydrothermalism temperature. Moreover, the absence of F in these rims corroborate the hypotheses of F depletion or incorporation in the lattice of elpidite. If the late fluid contained some F, it should be expected that some REE-fluoride could be identified.

Thereby, the sequence of the mineral crystallization of the Ouro Fino Intrusive Suite is proposed in the fig. 4.13. Given the inclusions of K-feldpar in the amphiboles, it is assumed that microcline was formed in the early magmatic stages. The arfvedsonite formed in the sequence followed by the aegirine on its rims. The existence of ferro-eckermannite in the Ouro Fino Intrusive Suite is still not well understood. If an albitization took place in the late stages of magmatism, the ferro-eckermannite could be the result of incorporation of Al_2O_3 by the Na-amphiboles. But this hypothesis is still constricted by the need for further studies.

The existence of anhedric and fine grained elpidite in clusters that resemble pseudomorpohs of elpidite sustain the possibility of primary elpidite instead of zircon. Thus,

zircon and Ca-elpidite formed in the hydrothermal stages. The existence of titanite in the rock beside zircons in the interstitial spaces could only explain a hydrothermal origin.

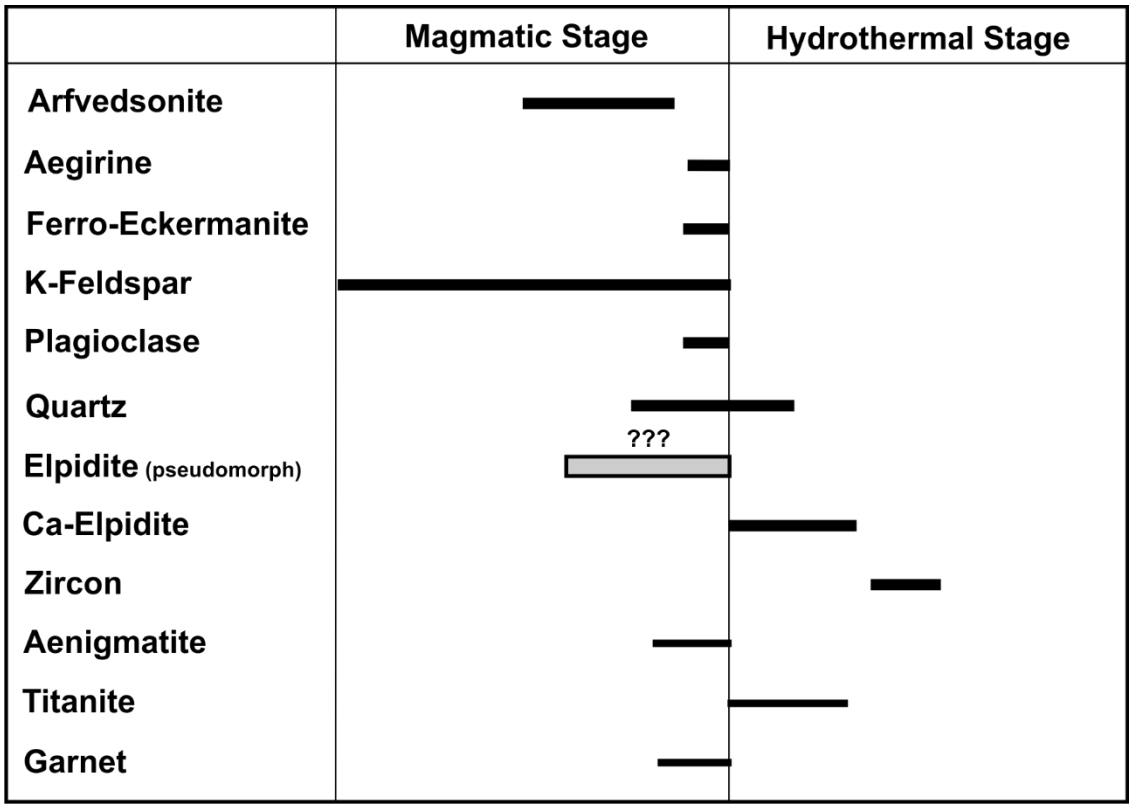

Figure 4.13: Mineral paragenesis evolution sequence of the Ouro Fino Intrusive Suite.

4.11. Conclusion

This study identifies the existence of three different alkaline intrusive suites in the Serra Grande Hill. Even though the São Domingos (1057 ± 10 Ma) and the Costa Marques intrusive (998 ± 10 Ma) suites intrude the Ouro Fino Intrusive Suite (1347 ± 9Ma), the petrographic and geochemical data advocate that the REE-Zr mineralization is factually associated to the most anciet of them.

The Ouro Fino Intrusive Suite is a hypesolvus alkaline granite, being microcline the first mineral to crystallize, and followed by the arfvedsonite. The substitution of arfvedsonite to aegirine in the amphibole rimes and also eventual rims of plagioclase on microcline rims are evidence of a Na enrichment during the crystallization.

The REE-Zr mineralization of the Ouro Fino Intrusive Suites is associated mainly with elpidite and zircon and subordinately with titanite. The crystallisation of the zirconosilicates seems to happen in the late-crystallization processes, with elpidite, titanite

and specially zircon occupying interstices of the rock. The formation of elpidite and zircon might be associated with pre-existing high contents of Zr, REE and Na in the magma, whereas titanite can be the metasomatic product of aenigmatite and Ca depletion from amphiboles.

The present study did not identify fluorides, carbonates and sulphides associated with the mineralization. The REE fractionation from the magma is possibly a product of incorporation of REE in the lattice of elpidite, titanite and specially zircon. The existence of an amorphous mass rich on Ce and La around of zircon crystals propones that REE also concentrated by the cooling of the hydrothermal system. There is a clear enrichment of LREE compared to HREE, being the average Lan/Ybn ≈ 8.

The existence of pseudomorphos of primary elpidite defines the Ouro Fino magmatism as agpaitic, allied to its clear peralkaline character. Similar examples of REE-Zr mineralization are Strange Lake, in Canadá and, Khan Bogd and Khaldzan Buregtey, both in Mongolia.

4.12. .Acknowledgements

“This work would not be possible without the encouragement of Prof. Bernhard Manfred Bühn. His support and contributions permitted the understanding of this mineralization, up to date unique in Brazil.’’

4.13. Appendix I (related to published article)

The chemical composition of minerals from samples CM-20A, CM-28, CM-31 and CM-39 were analyzed with a JEOL JXA-8530F field emission microprobe at BGR. Acceleration voltage and sample current are set to 20 kV and 40 nA, respectively and a beam width of 10 µm. For analysis the following respective X-ray line, standard, peak measuring time, and analyzing crystal were used: Na Kα, jadeite, 10 s; Mg Kα, diopside, 10 s; Al Kα, jadeite, 10 s; Si Kα, jadeite, 10 s; K Kα, orthoclase, 10 s; Ca Kα, diopside, 10 s; Ti Kα, rutile, 20 s; Mn Kα, rhodonite, 30 s; Fe Kα, almandine, 10 s; Sr Lα, coelestine, 30 s,; Y Lα, synthetic zirconia, 30 s; Zr Lα, zircon, 60 s; La Lα, monazite, 60 s; Ce Lα, monazite, 50 s; Hf Lα, synthetic zirconia, 50 s.

Samples CM-18 and CM-20B were analysed with a JEOL JXA-8230 field emission microprobe at LME-IG in three different proceedings. First proceeding (i) was performed

for the chemical composition of amphiboles and pyroxenes. The second (ii) was made aiming to analyse major elements in minerals that are potential hosts for REE. The third (iii) was made to measure REE content in amphiboles, pyroxenes and minerals that are potential hosts for REE, herein defined as zircon, titanite and elpidite.

(i) First proceeding, the analysed elements are F, Al, Si, Ca, K, Cl, Ti, Cr, Mn, Sr, Ni, Fe, V and B. The analyses were performed with sample current of 10 nA and voltage acceleration of 15 kV, and peak measuring time of 10 s. The utilized lines and respective detected the elements are Kα – Na, F, Al, Si, Ca, K, Cl, Ti, Cr, Mn, Ni, Fe, and V; Lα – Ba, Sr.

(ii) In the second proceeding, the analysed elements are F, Al, Si, P, Nb, Mn, Ti, Y, Ta, Ca, Fe and Zr. The assay was made with a sample current of 10 nA and voltage acceleration of 15 kV, with peak measuring time of 10 s. The applied lines for the elements are Kα – F, Al, Si, P, Mn and Ti; Lα – Y; Kβ – Ca; and Lβ – Nb and Zr.

(iii) The third assay analysed the REE plus Na, K, U, Th and Ba. The proceeding was conducted with voltage acceleration of 20 kV, sample current of 50 nA and peak measuring time of 10 s. The utilized lines and respective elements are Kα – Na and K; Lα – La, Ce, Nd, Eu, Gd, Tb, Er, Tm, Yb, Lu and Ba, Lβ – Ho, Sm, Dy and Pr**.**

For all the analyses, the used beam had 10 µm of width.

5. REFERENCES

ALS Global. (2018). Schedule of Services & Fee. Vancouver. Retrieved from https://www.alsglobal.com/ca/myals/downloads?keywords=Geochemistry+Fee+Schedule&category=b5b5208b58bc4609bd2fa20f32d820f8

Bettencourt, J.S.; R.M. Tosdal, R.M.; W.B. Leite Jr, W.B.; Payolla, B.L. (1999). Mesoproterozoic rapakivi granites of the Rondônia Tin Province, southwestern border of the Amazonian craton, Brazil — I. Reconnaissance U–Pb geochronology and regional implications. Precambrian Research, 95(1–2), 41–67.

Bettencourt, J.S; Leite Jr. W.B; Ruiz, A.S.; Matos, R.; Payolla, B.L.; R. M. T. (2010). The Rondonian-San Ignacio Province in the SW Amazonian Craton: An overview,

Journal of South American Earth Sciences. Journal of South American Earth Sciences, 29(1), 28–46. Retrieved from

Bettencourt, J.S.; Leite Júnior, W.B.; Payolla, B.L.; Crespo, D.G; Sato, K. (2012). Três suítes magmáticas distintas na região de Costa Marques, SW de Rondônia: resultados preliminares. In 46oCongresso Brasileiro de Geologia. Salvador: SBG.

Bettencourt, Jorge Silva; Payolla, Bruno Leonelo; Leite Júnior, Washington Barbosa; Sato, Kei; Basei, M. A. S. (2014). Paleo- to Mesoproterozoic crustal sources for the igneous felsic rocks of the Costa Marques region, SW Amazonian Craton, Brazil:: evidence from preliminary SHRIMP U-Pb zircon ages and Hf isotopes in zircon. In 9th SSAGI: Program and Abstracts. São Paulo: Instituto de Geociências - USP.

Bettencourt, J. S., Leite, W. B., Ruiz, A. S., Matos, R., Payolla, B. L., & Tosdal, R. M. (2010). The Rondonian-San Ignacio Province in the SW Amazonian Craton: An overview. Journal of South American Earth Sciences, 29(1), 28–46. https://doi.org/https://doi.org/10.1016/j.jsames.2009.08.006

Boynton, W. V. (1984). Geochemistry of the rare earth elements: meteorite studies. In P. Henderson (Ed.), Rare earth element geochemistry. (pp. 63–114). Eksevier.

Buch, T., Chemale, L. T., Silva, G. F. da, & Oliveira Neto, W. L. de. (2018). No Title Ocorrências de elementos terras raras em rochas alcalinas da suíte Ouro Fino, Costa Marques, Rondônia, Brasil: descrição e modelo para prospecção geofísica e geoquímica. Brasília: CPRM.

Chakhmouradian, A., & Zaitsev, A. (2012). Rare Earth Mineralization in Igneous Rocks: Sources and Processes. Elements (Vol. 8). https://doi.org/10.2113/gselements.8.5.347

Cordani, U. G., & Teixeira, W. (2007). Proterozoic accretionary belts in the Amazonian Craton . The Geological Society of America, Special Publications, 200(303), 297–320. https://doi.org/10.1130/2007.1200(14)

Costa, E. G. da. (1990). Projeto Costa Marques - Relatório da Fase de Prospecção Preliminar. Porto Velho.

CPRM. (2010). Projeto Aerogeofísico Sudoeste de Rondônia: relatório final do levantamento e processamento dos dados magnetométricos e gamaespectrométricos. Rio de Janeiro.

Dostal, J. (2017). Rare Earth Element Deposits of Alkaline Igneous Rocks. Resources (Vol. 6). https://doi.org/10.3390/resources6030034

Eby, G. N. (1992). Chemical subdivision of the A-type granitoids:Petrogenetic and tectonic implications. Geology, 20(7), 641. https://doi.org/10.1130/0091-7613(1992)020<0641:CSOTAT>2.3.CO;2

Freitas, A. F. de; S. J. R. A. B. V. (1985). Projeto Mapas Metalogenéticos e de Previsão de Recursos Minerais - Folha SD.20 Guaporé - Escala 1:100.000 (No. 1753). Porto Velho.

Frost, B.R., Barnes, C.G., Collins, W.J., Arculus, R.J., Ellis, D.J., Frost, C. D. (2001). A geochemical classification for granitic rocks. Journal of Petrology, 42, 2033–2048.

Grigor'eva, A.A., Zubkova, N., Pekov, I., Kolitsch, U., Dmitry, P., Vigasina, M., Chukanov, N. (2011). Crystal Chemistry of Elpidite from Khan Bogdo (Mongolia) and Its K- and Rb-Exchanged Forms. Crystallography Reports - CRYSTALLOGR REP (Vol. 56).

Gysi, A. P., & Williams-Jones, A. E. (2013). Hydrothermal mobilization of pegmatite-hosted REE and Zr at Strange Lake, Canada: A reaction path model. Geochimica et Cosmochimica Acta, 122(Supplement C), 324–352. https://doi.org/https://doi.org/10.1016/j.gca.2013.08.031

Isotta, C.A.L., Carneiro, J.M., Kato, H.T., Barros, R. J. L. (1978). Projeto Província Estanífera de Rondônia. Porto Velho.

Kovalenko, V. I. (1995). The peralkaline granite-related Khaldzan-Buregtey rare metal (Zr, Nb, REE) deposit, western Mongolia. Economic Geology, 90(3), 530–547. https://doi.org/10.2113/gsecongeo.90.3.530

Kynicky, J., Chakhmouradian, A. R., Xu, C., Krmicek, L., & Galiova, M. (2011a). Distribution and evolution of zirconium mineralization in peralkaline granites and associated pegmatites of the Khan Bogd complex, southern Mongolia. Canadian Mineralogist, 49(4), 947–965.

Maniar, P. D. & Piccoli, P.M. (1989). Tectonic discrimination of granitoids. Geological Society of America Bulletin, 101, 635–643.

Marks, M. A. W., & Markl, G. (2017). A global review on agpaitic rocks. Earth-Science Reviews, 173(Supplement C), 229–258.

Migdisov, A., Williams-Jones, A. E., Brugger, J., & Caporuscio, F. A. (2016). Hydrothermal transport, deposition, and fractionation of the REE: Experimental data and thermodynamic calculations. Chemical Geology.

Paulick, H., & Machacek, E. (2017). The global rare earth element exploration boom: An analysis of resources outside of China and discussion of development perspectives. Resources Policy, 52, 134–153.

Payolla, B. L.; Leite Júnior, W. B.; Bettencourt, J. S. (2013). Litogeoquímica de rochas ígneas félsicas da região de Costa Marques, SW de Rondônia: considerações preliminares. In XIV Congresso Brasileiro de Geoquímica. Diamantina: Anais do XIV Congresso Brasileiro de Geoquímica.

Priem H.N.A., Boelrijk N.A.I.M., Hebeda E.H., Verdurmen E.A.Th., Verschure R.H., B. E. H. (1971). Granitic complexes and associated tin mineralizations of “Grenville” age in Rondônia, western Brazil. Geological Society of America Bulletin, (82), 1095–1102.

Quadros, M.L. do E.S.; Rizzotto, G. J. (2007). Geologia e Recursos Minerais do Estado de Rondônia: Sistema de Informações Geográficas-SIG. Programa Geologia do Brasil (PGB), Integração, Atualização e Difusão de Dados da Geologia do Brasil, Subprograma Mapas Geológicos Estaduais. Porto Velho.

Rizzotto, G. J., Quadros, M., Bahia, R. B., Dall’Igna, L. G., & Cordeiro, A. V. (2004). Folha SD.20 - Guaporé. In C. et al. Schobbenhaus (Ed.), Carta Geológica do Brasil ao Milionésimo, SIstemas de Informações Geográficas. Programa Geologia do Brasil. Brasília: CPRM.

Rizzotto, G. J. (2010). Geologia e recursos minerais da folha Pimenteiras SD.20-X-D. Porto Velho.

Rizzotto, G. J., Hartmann, L. A., Santos, J. O. S., & Mcnaughton, N. J. (2014). Tectonic evolution of the southern margin of the amazonian craton in the late mesoproterozoic based on field relationships and zircon U-Pb geochronology. Anais Da Academia Brasileira de Ciencias, 86(1), 57–84.

Rizzotto, G. J., Santos, J. O. S., Hartmann, L. A., Tohver, E., Pimentel, M. M., & McNaughton, N. J. (2013). The Mesoproterozoic Guaporé suture in the SW Amazonian Craton: Geotectonic implications based on field geology, zircon geochronology and Nd–Sr isotope geochemistry. Journal of South American Earth Sciences, 48(Supplement C), 271–295.

Salvi, S., & Williams-Jones, A. E. (1990). The role of hydrothermal processes in the granite-hosted Zr, Y, REE deposit at Strange Lake, Quebec/Labrador: Evidence from fluid inclusions. Geochimica et Cosmochimica Acta, 54(9), 2403–2418.

Salvi, S., & Williams-Jones, A. E. (1995). Zirconosilicate phase relations in the Strange Lake (Lac Brisson) pluton, Quebec-Labrador, Canada. American Mineralogist, 80(9–10), 1031–1040.

Santos, R.O.B.; Pitthan, J.H.L.; Barbosa, E.S.; Fernandes, C.A.C.; Tassinari, C.C.G.; Campos, D. . (1979). Geologia. In Projeto Radam Brasil. Folha SD.20 Guaporé (Levantamen, pp. 21–123). Rio de Janeiro: MME/DNPM.

Sayão Lobato, F.P.N.; Appel, L.E.; Godoy, M. C. F. de et al. (1966). Pesquisa de cassiterita no território federal de Rondônia. Relatório Final. Rio de Janeiro.

Scandolara, J. E. (1999). Geologia e Recursos Minerais do Estado de Rondônia. Rio De Janeiro.

Tassinari, C. C. G., & Macambira, M. J. B. (1999). Geochronological provinces of the Amazonian Craton. Episodes, 22(3), 174–182.

Thompson, R. N. (1982). Magmatism of the British Tertiary Volcanic Province. Scottish Journal of Geology, 18(1), 49–107.

Torres, L. C. A. (1979). Projeto Sudoeste de Rondônia. Relatório Final. Porto Velho.

Wall, F. (2014). Rare earth elements. In Critical Metals Handbook (pp. 312–339). John Wiley & Sons.

Whalen, J.B.; Currier, K.L.; Chappel, B. W. (1987). A-type granites: geochemical characteristics, discrimination and petrogenesis. Contrib. Mineral. Petrol., (95), 407–419.

6. APPENDIX I

Table 1: Modal mineralogy and considered chemical formulas for the rocks of Ouro Fino Intrusive Suite.

Ouro Fino Intrusive Suite

Proportion	Mineral	Formula
40-60	Microcline	$KAlSi_3O_8$
15-25	Arfvesdsonite	$Na_3(Fe^{2+}4Fe^{3+})Si_8O_{22}(OH)_2$
5-15	Quartz	SiO_2
5-10	Elpidite	$Na_2ZrSi_6O_{15}•3(H2O)$
1-5	Albite – Oligoclase	$Na_{(1-0.7)}\ Ca_{(0.3-0)}\ AlSi3O8$
1-5	Aegirine	NaFeSi2O6
acessory	Aenigmatite	$Na_2Fe^{2+}{}_5TiSi_6O_{20}$
acessory	Zircon	$ZrSiO_4$
acessory	Analcime	$NaAl(Si_2O_6)•(H_2O)$
acessory	Garnet	$Fe^{2+}{}_3Al2(SiO_4)_3$
acessory	Titanite	$CaTiSiO_5$
acessory	Iron Oxide	FeO

Table 2: Rock powder XRD results for the samples CM-31 (fmg) and CM-39(cmg).

Mineral	**Ideal Chemical Formula**	**Samples**	
		OFIS – fine graiend	OFIS – coarse grained
Quartz	SiO2	31.1	31.4
Albite	NaAlSi3O8	18.9	23.5
Microcline	KAlSi3O8	23.1	22.0
Aegirine	NaFeSi2O6	18.3	6.8
Ferro-Eckermannite	Na3(Fe4Al)Si8O22(OH)2	8.6	16.4
Total		100.0	100.0

Table 3: Chemical results from the samples of the Costa Marques (CMIS), São Domingos (SDIS) and Ouro Fino (OFIS) intrusive suites.

Suite	OFIS													SDIS		CMIS		
Sample	CM-02	CM-04	CM-16	CM-18	CM-20	CM-22B	CM-28C	CM-39	CM-17	CM-28A	CM-31	CM-33B	CM-22A	CM-13	CM-25A	CM-09	CM-10	CM-40
	cmg	cmg	cmg	cmg	cmg	cmg	cmg	cmg	mg	fmg	fmg	cmg	trachyte	afg	akf	trachyte	basalt	trachyte
SiO2	71.60	71.70	70.00	70.90	69.30	69.10	72.00	68.80	75.10	69.40	70.40	73.40	74.80	67.10	69.80	58.40	43.90	58.20
Al2O3	10.10	7.83	5.38	7.34	8.49	7.29	8.15	8.16	6.62	8.17	7.52	7.22	5.95	14.30	10.40	12.95	15.05	15.05
Fe2O3	7.10	9.76	11.45	11.05	10.05	12.25	9.12	10.50	8.82	9.71	9.13	7.78	7.76	5.31	6.87	13.00	13.60	11.35
CaO	0.41	0.42	0.78	0.41	0.64	0.32	0.53	0.51	0.37	0.44	0.41	1.26	0.47	1.20	0.50	3.52	7.99	2.27
MgO	0.06	0.11	0.04	0.05	0.07	0.01	0.03	0.24	0.01	0.07	0.02	0.06	0.01	0.33	0.07	0.51	5.25	0.39
Na2O	4.39	3.96	3.83	4.57	4.44	4.21	4.29	4.62	6.98	4.34	4.83	5.17	3.49	5.41	4.70	4.19	3.03	4.79
K2O	5.26	4.53	3.63	4.25	4.66	4.43	4.89	4.35	1.20	4.36	4.05	3.42	5.09	5.38	4.44	4.38	1.14	5.10
Cr2O3	0.01	0.01	0.01	0.01	0.01	0.01	0.01	0.01	0.01	0.01	0.01	0.01	0.01	0.01	0.01	0.01	0.01	0.01
TiO2	0.21	0.41	0.60	0.29	0.39	0.29	0.53	0.41	0.36	0.41	0.49	0.45	0.51	0.36	0.38	1.21	2.45	1.17
MnO	0.13	0.16	0.23	0.20	0.23	0.20	0.16	0.16	0.09	0.20	0.16	0.30	0.20	0.14	0.14	0.35	0.23	0.19
P2O5	0.03	0.02	0.07	0.03	0.04	0.02	0.05	0.02	0.09	0.01	0.07	0.10	0.22	0.04	0.03	0.35	0.62	0.31
SrO	0.01	0.01	0.01	0.01	0.01	0.01	0.01	0.01	0.01	0.01	0.01	0.01	0.01	0.01	0.01	0.01	0.03	0.01
BaO	0.01	0.01	0.02	0.01	0.01	0.01	0.01	0.01	0.01	0.01	0.01	0.01	0.01	0.07	0.05	0.05	0.08	0.13
LOI	0.69	0.86	2.29	0.72	1.11	1.07	1.04	1.19	1.11	0.98	1.26	1.61	1.33	1.27	0.66	1.58	6.29	1.66
Total	99.98	99.77	98.33	99.82	99.45	99.19	100.8	98.97	100.75	98.1	98.35	100.79	99.84	100.92	98.05	100.5	99.67	100.62
La	1175	582	2470	526	2600	816	2070	1190	1540	1640	1165	1960	1785	804	1045	100	21	114.5
Ce	2460	1735	4660	1895	2660	1315	2470	1975	3150	3280	2660	4000	4080	1480	1685	241	56.2	261
Pr	369	207	915	164.5	873	237	555	473	439	443	310	499	460	175	283	28.7	7.36	37.3
Nd	1480	848	3600	638	3340	964	2110	1660	1685	1695	1130	1770	1670	693	1095	124	35.9	152
Sm	300	188	729	147	583	205	416	294	349	352	205	313	341	129	230	25.2	9.15	32.1
Eu	18.95	14.4	47.4	11.35	35.5	14.25	29	20.1	26.1	25	14.4	21.8	23.9	9.06	17.85	3.64	2.95	5.78
Gd	250	195	567	152	464	199.5	379	258	356	327	186	280	320	108.5	228	24.9	9.45	33.4
Tb	42.4	36.5	88	29.1	65.6	29.4	56.7	40.6	54.6	51.8	29.7	43.3	54.4	15.8	35.9	3.86	1.39	5.16
Dy	231	214	478	182	346	163	322	242	321	292	167.5	240	322	84.2	205	23	8.32	28.8
Ho	46.9	45.3	84.3	36.3	61.5	31.5	58.7	46	60.5	52.3	30.8	45.6	60.5	15.25	39	4.48	1.66	5.41
Er	139	140	239	113.5	161.5	88.6	162	140	176.5	146.5	89.9	128	176.5	40.1	109.5	13.2	4.76	15.2
Tm	19.55	19.75	31.3	16.95	21.1	11.4	22.3	20.2	24	20.3	12.9	16.35	23.3	5.11	14.2	1.85	0.63	2.06
Yb	123	121	194	115.5	127	71.8	139.5	132.5	150	135.5	83	96.8	144	32.4	85.4	11	4.04	13.25
Lu	16.85	16.45	24.7	15.8	17	10.05	18.15	18.15	19.6	18.6	11.1	12.4	18.55	4.41	11.8	1.88	0.61	2.01
Y	1010	1155	1790	839	1305	771	1270	1085	1545	975	816	1635	1720	460	1055	112.5	43	138
Cr	30	30	0	10	10	0	10	0	10	10	20	10	40	30	10	50	60	5
V	8	6	10	7	7	9	2.5	10	9	9	6	11	8	10	7	11	210	7
Ba	37.5	45	158.5	51.8	74	31	111.5	57.5	54.9	95.5	120.5	118	79.7	614	510	420	733	1155
Cs	0.94	0.77	1.84	0.6	0.94	0.39	0.36	0.39	0.39	0.5	0.56	0.4	0.85	1.48	0.43	3.15	1.01	0.4
Rb	506	485	477	380	404	417	501	356	87.2	471	502	407	577	232	319	79.6	26.6	84.7
Sr	13.9	12.5	64.3	13.5	15.3	4.4	25	20.7	31.9	17.8	21.8	53	30.4	60.4	43.5	73.5	292	124
Ga	82.9	67.8	72.2	64.4	83.8	69.8	74.2	73	90	73.9	75	75.1	68	58.4	63.5	39.1	29.2	34.8
Hf	245	384	393	324	314	196.5	253	305	318	247	238	205	278	41.4	175	32.2	6.8	31.9
Zr	9250	>10000	>10000	>10000	>10000	7380	9420	>10000	>10000	8840	9420	8430	>10000	1500	6260	1320	255	1410
W	1	2	2	2	2	1	2	1	2	1	1	1	0.5	2	1	1	2	1
Nb	263	308	425	293	256	181.5	350	319	442	312	890	808	778	89.2	184	31.5	5.8	31.2
Ta	17.9	22.2	41.4	19.1	18.6	9.5	21	19.7	30.8	20.3	21.5	24.8	30.3	3.8	10.5	1.6	0.4	1.6
Sn	55	89	172	68	56	48	73	66	127	72	149	163	187	22	46	4	2	5
Th	44.5	61.4	53.4	55	40.7	27.5	51.4	40.9	71.9	56.7	176	318	209	31.8	33.9	5.37	0.72	4.9
U	18.9	27.9	29.7	25.2	20.6	15.95	24.5	22.4	39.6	22.3	81	119.5	69.9	10.15	17.3	1.78	0.25	1.06
TREO(%)	0.78	0.51	1.65	0.47	1.33	0.48	1.03	0.76	0.97	0.99	0.71	1.10	1.11	0.42	0.59	0.07	0.02	0.08
(La/Yb)n	6.44	3.24	8.58	3.07	13.80	7.66	10.00	6.06	6.92	8.16	9.46	13.65	8.36	16.73	8.25	6.13	3.50	5.83

Table 4: Mineral chemistry results for the Na-amphiboles and Na-pyroxenes from the samples CM-18, CM-20A, CM-20B, CM-28C, CM-31 and CM-39. Abreviations for mineral names: fee = ferro-eckermannite; arf = arfvedsonite; far = fluor-arfvedsonite; aeg = aegirine. Abbreviations: n.a. = not analysed; n.d. = not detected.

Sample	CM20A					CM-20B	CM-28C	CM-31	CM-20B	CM-28C	CM-31	CM-39	CM18
Mineral	fee	arf	far	arf					aeg				
SiO_2	49.1	49.1	49.0	49.3	49.2	50.1	49.6	49.7	52.2	51.8	51.3	52.9	51.3
TiO_2	1.36	1.73	1.59	1.35	1.60	1.51	1.40	1.33	0.72	1.17	2.02	1.03	0.06
Al_2O_3	0.33	0.28	0.32	0.24	0.41	0.18	0.21	0.13	0.30	0.25	0.04	0.54	0.08
FeO	32.3	32.2	31.1	32.8	32	30.5	29.8	31.6	All Fe as Fe_2O_3				
Fe_2O_3	1.76	1.71	3.7	1.56	1.91	1.38	1.86	2.31	33.2	32.4	29.4	31.4	29.4
MgO	0.10	0.29	0.24	0.08	0.18	1.60	1.75	0.02	n.d.	0.05	n.d.	0.07	n.d.
MnO	0.79	0.66	0.66	0.72	0.69	0.63	0.62	0.61	0.05	0.06	1.15	0.46	1.12
CaO	2.00	2.01	1.59	2.02	1.36	1.57	1.61	0.52	0.27	0.34	2.78	0.73	0.07
Na_2O	7.53	7.68	8.04	7.56	7.83	7.54	7.54	8.09	12.6	12.6	11.1	12.6	13.4
K_2O	1.67	1.53	1.56	1.58	1.69	1.69	1.57	1.55	n.d.	n.d.	n.d.	n.d.	0.03
ZrO_2	n.a.	n.a.	n.a.	n.a.	n.a.	0.09	0.05	0.08	0.04	0.07	1.8	0.04	n.a.
HfO_2	n.a.	n.a.	n.a.	n.a.	n.a.	n.d.	n.d.	n.d.	n.d.	n.d.	n.d.	n.d.	n.a.
F	1.91	1.87	2.00	1.58	1.44	n.a.	n.a.	n.a.	n.a.	n.a.	n.a.	n.a.	n.d.
Cl	n.d.	0.01	0.01	0.01	0.03	n.a.	n.a.	n.a.	n.a.	n.a.	n.a.	n.a.	n.d.
BaO	n.d.	0.04	n.d.	n.d.	n.d.	n.a.	n.a.	n.a.	n.a.	n.a.	n.a.	n.a.	n.d.
NiO	0.00	0.04	n.d.	n.d.	n.d.	n.a.	n.a.	n.a.	n.a.	n.a.	n.a.	n.a.	n.d.
Cr_2O_3	n.d.	n.d.	0.02	n.d.	0.06	n.a.	n.a.	n.a.	n.a.	n.a.	n.a.	n.a.	0.03
V_2O_3	n.d.	n.d.	n.d.	0.01	0.00	n.a.	n.a.	n.a.	n.a.	n.a.	n.a.	n.a.	n.d.
SrO	0.04	n.d.	0.15	n.d.	0.03	n.d.	n.d.	n.d.	n.d.	n.d.	n.d.	n.d.	n.d.
La_2O_3	n.a.	n.a.	n.a.	n.a.	n.a.	n.d.	n.d.	n.d.	0.01	n.d.	0.02	n.d.	n.a.
Ce_2O_3	n.a.	n.a.	n.a.	n.a.	n.a.	0.01	0.02	n.d.	n.d.	0.01	0.08	n.d.	n.a.
Total	98.7	99.1	100.1	98.71	98.4	96.86	96.19	96.01	99.18	98.98	99.69	99.7	95.5

Table 5: Mineral chemistry results for the zircons and titanite found in the samples CM-20A, CM-39, CM-18, CM-20B and CM-28. Abbreviations: n.a. = not analysed; n.d. = not detected.

	Zircon										**Titanite**				
Sample	CM20A						CM39				CM18	CM-20B	CM-20B	CM-28	
Spot							39/1	39/2	39/4	39/3					
SiO_2	30.68	32.22	30.68	30.65	31.29	30.04	30.54	30.71	29.28	29.61	29.05	28.45	30.06	30.08	29.58
TiO_2	0.14	n.d	0.14	0.02	0.28	0.26	0.15	0.19	0.20	0.21	33.56	37.38	36.12	38.52	38.03
$Al2O_3$	0.14	0.16	0.14	0.20	0.17	0.22	0.22	0.28	0.25	0.27	0.40	0.05	0.16	0.06	0.08
FeO	all Fe as Fe_2O_3														
Fe_2O_3	0.30	0.24	0.30	0.19	0.31	0.47	0.72	0.61	0.68	0.87	2.77	1.23	3.65	1.15	2.54
MgO	n.a.	n.a.	n.a.	n.a.	n.a.	n.a.	n.d	n.d	n.d	n.d	n.a.	n.d.	n.d.	n.d.	n.d.
MnO	0.07	0.05	0.07	0.09	0.23	0.35	0.49	0.22	0.47	0.62	n.d	n.d	n.d	n.d	n.d
CaO	0.75	0.55	0.75	0.56	0.77	1.10	0.77	0.72	0.91	0.95	27.33	21.19	26.96	26.03	26.03
Na_2O	0.08	n.d	0.08	0.03	0.17	0.11	n.d	n.d	n.d	n.d	0.37	1.86	0.20	0.71	0.34
K2O	0.02	0.02	0.02	n.d	n.d	0.02	0.02	0.02	0.02	0.03	0.01	n.d.	0.01	0.01	n.d
ZrO_2	59.8	59.1	59.8	56.5	56.9	56.1	53.7	53.5	51.6	51.1	0.24	0.19	0.30	0.25	0.14
Nb_2O_5	0.74	0.60	0.74	0.75	0.73	0.95	n.a.	n.a.	n.a.	n.a.	1.66	n.a.	n.a.	n.a.	n.a.
Ta_2O_5	0.08	0.01	0.08	0.07	0.08	0.19	n.a.	n.a.	n.a.	n.a.	0.26	n.a.	n.a.	n.a.	n.a.
HfO_2	1.49	0.94	1.49	1.11	0.82	0.93	1.11	1.39	1.17	0.98	n.d.	0.02	n.d	n.d	n.d
P_2O_5	0.12	n.d.	0.12	0.02	n.d.	0.04	n.a.	n.a.	n.a.	n.a.	0.06	n.a.	n.a.	n.a.	n.a.
F	n.d.	0.01	n.d.	n.d.	n.d.	n.d.	n.a.	n.a.	n.a.	n.a.	0.03	n.a.	n.a.	n.a.	n.a.
PbO	n.d.	n.d.	n.d.	n.d.	n.d.	n.d.	n.a.	n.a.	n.a.	n.a	n.d	n.a.	n.a.	n.a.	n.a.
SrO	0.29	0.14	0.29	0.06	0.23	0.31	n.d	n.d	n.d	n.d	n.d	n.d	n.d	n.d	n.d
BaO	n.d	0.08	n.d	0.05	0.06	0.08	n.a.	n.a.	n.a.	n.a.	0.07	n.a	n.a	n.a	n.a
ThO2	n.d.	n.d.	n.d.	0.15	0.10	n.d.	n.a.	n.a.	n.a.	n.a.	0.04	n.a	n.a	n.a	n.a
UO2	0.15	0.22	0.15	0.26	0.22	0.29	n.a.	n.a.	n.a.	n.a.	0.16	n.a	n.a	n.a	n.a
La_2O_3	0.08	0.17	0.08	0.09	0.09	0.25	0.34	0.38	0.34	0.33	0.08	0.22	0.01	0.02	0.06
Ce_2O_3	1.84	0.77	1.84	4.19	1.00	1.43	1.28	1.33	1.24	1.47	0.54	0.76	n.d	n.d	0.20
Pr_2O_3	0.12	n.d.	0.12	n.d.	n.d.	0.18	n.a.	n.a.	n.a.	n.a.	0.02	n.a.	n.a	n.a	n.a
Sm_2O_3	0.03	0.20	0.03	0.07	0.21	0.28	n.a.	n.a.	n.a.	n.a.	n.d.	n.a.	n.a	n.a	n.a
Nd_2O_3	0.20	0.22	0.20	0.34	0.31	0.22	n.a.	n.a.	n.a.	n.a.	0.01	n.a.	n.a	n.a	n.a
Eu_2O_3	0.17	0.09	0.17	0.03	0.12	0.10	n.a.	n.a.	n.a.	n.a.	0.09	n.a.	n.a	n.a	n.a
Gd_2O_3	0.15	0.06	0.15	0.41	0.18	0.12	n.a.	n.a.	n.a.	n.a.	0.01	n.a.	n.a	n.a	n.a
Tb_2O_3	n.d.	n.d.	n.d.	n.d.	n.d.	n.d.	n.a.	n.a.	n.a.	n.a.	n.d.	n.a.	n.a	n.a	n.a
Dy_2O_3	0.01	0.14	0.01	0.12	0.17	0.05	n.a.	n.a.	n.a.	n.a.	n.d.	n.a.	n.a	n.a	n.a
Ho_2O_3	n.d.	n.d.	n.d.	n.d.	n.d.	0.46	n.a.	n.a.	n.a.	n.a.	n.d.	n.a.	n.a	n.a	n.a
Er_2O_3	0.28	0.22	0.28	0.28	0.39	0.03	n.a.	n.a.	n.a.	n.a.	0.03	n.a.	n.a	n.a	n.a
Tm_2O_3	n.d.	0.08	n.d.	0.12	n.d.	n.d.	n.a.	n.a.	n.a.	n.a.	n.d.	n.a.	n.a	n.a	n.a
Yb_2O_3	0.18	0.05	0.18	0.12	0.17	n.d	n.a.	n.a.	n.a.	n.a.	n.d.	n.a.	n.a	n.a	n.a
Lu_2O_3	n.d.	0.23	n.d.	0.01	0.17	n.d.	n.a.	n.a.	n.a.	n.a.	n.d.	n.a.	n.a	n.a	n.a
Y_2O_3	0.31	1.05	0.31	1.59	1.90	2.03	2.55	2.48	3.25	3.42	0.31	2.55	0.63	0.29	1.18

TREO+Y	3.37	3.28	3.37	7.37	4.71	5.15	4.17	4.19	4.83	5.22	1.08	3.53	0.64	0.31	1.44
Total	98.28	97.63	98.28	98.06	97.16	96.68	91.94	91.89	89.46	89.88	97.09	93.90	98.10	97.12	98.18

Table 6: Mineral chemistry results for elpidite found in thin-sections from samples CM-20B, CM-28C, CM-31 and CM-39. The spots 31/1 and 31/2 are shown in Fig. 10.C and 10.D.

Elpidite

Spot						**31/1**	**31 / 2**				
Sample	CM-20B	CM-28	CM-28	CM-31	CM-31	CM-31	CM-31	CM-39	CM-39	CM-39	CM-39
SiO_2	62,68	65,99	63,52	63,88	62,03	61,12	63,67	66,81	66,44	64,96	66,07
TiO_2	0,15	n.d	0,02	n.d	n.d	0,03	0,02	n.d	n.d	0,19	0,03
Al_2O_3	0,04	0,07	0,04	0,06	0,03	0,04	0,05	0,02	0,02	0,03	0,02
FeO	0,29	0,57	0,69	0,85	1,30	0,95	0,69	0,33	0,40	0,29	0,22
Fe_2O_3	All Fe as FeO										
MgO	n.d	n.d	n.d	n.d	n.d	n.d	n.d	0,02	n.d	n.d	n.d
MnO	0,05	0,09	0,21	0,11	0,19	0,33	0,10	0,04	0,02	0,02	0,05
CaO	1,57	1,42	2,88	2,12	3,01	3,00	2,22	1,11	0,89	0,31	0,74
Na_2O	1,55	4,67	2,87	2,43	1,05	1,11	2,46	5,26	4,79	5,61	4,89
K_2O	6,94	0,37	0,65	1,33	4,18	4,55	1,72	0,44	0,46	0,26	0,47
ZrO_2	19,30	21,02	18,90	19,74	18,91	18,25	19,20	21,20	21,82	21,44	21,06
HfO_2	0,44	0,42	0,34	0,40	0,38	0,37	0,41	0,53	0,58	0,47	0,38
SrO	n.d	n.d	n.d	n.d	n.d	n.d	n.d	n.d	n.d	n.d	n.d
La_2O_3	0,04	0,02	0,06	0,03	0,05	0,04	0,02	0,03	0,02	n.d	0,03
Ce_2O_3	n.d	n.d	0,03	0,03	0,04	0,04	n.d	0,04	n.d	n.d	n.d
Y_2O_3	1,08	0,67	1,92	1,07	1,41	1,49	1,44	0,48	0,22	0,09	0,83
TREO+Y	1,11	0,69	2,01	1,14	1,49	1,57	1,46	0,54	0,24	0,09	0,86
Total	94,13	95,32	92,12	92,07	92,57	91,32	92,00	96,29	95,64	93,67	94,80

Table 7: WDS results for the analysed zircon and the needles and mass rimming the crystals. The analysed spots are visible in figure 4.11.

Mineral	Zircon		
Spot	31/1	31/2	31/3
SiO_2	27.484	30.04	26.738
TiO_2	0	0.259	0
Al_2O_3	2.36	0.218	0.324
FeO	14.625	0.471	0.311
Fe_2O_3	-	-	-
MnO	0.363	0.352	0.088
CaO	10.997	1.096	0.364
Na_2O	0.039	0.112	0
K_2O	0.023	0.018	0.029
ZrO_2	7.233	56.173	38.316
Nb_2O_5	0	0.954	0.422
Ta_2O_5	0	0.186	0
HfO_2	0.218	0.929	0.722
P_2O_5	0.009	0.036	0.424
F	0	0	0
PbO	0.02	0	0
SrO	0.263	0.31	0
BaO	0.046	0.082	0
ThO_2	0.09	0	0.018
UO_2	0.109	0.286	0.191
La_2O_3	5.968	0.25	0.08
Ce_2O_3	8.102	1.428	13.288
Pr_2O_3	0.306	0.183	0.04
Sm_2O_3	0.011	0.276	0.526
Nd_2O_3	1.145	0.224	0.935
Eu_2O_3	0.115	0.101	0.225
Gd_2O_3	0.74	0.116	1.114
Tb_2O_3	0	0	0
Dy_2O_3	0	0.054	0.708
Ho_2O_3	0	0.457	0.408
Er_2O_3	0.062	0.03	0.493
Tm_2O_3	0.046	0	0.03
Yb_2O_3	0	0	0.614
Lu_2O_3	0.111	0	0.196
Y_2O_3	0.225	2.034	5.176
TREO+Y	16.831	5.153	23.833
Total	80.71	96.675	91.78

7. APPENDIX II

Table 8: Coordinates and analytical techniques of the studied samples. Abbreviations: OFIS: Ouro Fino Intrusive Suite; SDIS: São Domingos Intrusive Suite; CMIS: Costa Marques Intrusive Suite.

Samples	Lithotype	Subfacies	Analyses	Longitude	Latitude	DATUM
CM-02	OFIS	cmg	ICP-AES; ICP-MS	-64,34601038	-12,18603783	Sirgas 2000
CM-04	OFIS	cmg	ICP-AES; ICP-MS	-64,32858083	-12,1910062	Sirgas 2000
CM-09	CMIS	-	ICP-AES; ICP-MS	-64,29662536	-12,25712259	Sirgas 2000
CM-10	CMIS	-	ICP-AES; ICP-MS	-64,3030856	-12,25680137	Sirgas 2000
CM-13	SDIS	-	ICP-AES; ICP-MS	-64,32709614	-12,23029705	Sirgas 2000
CM-16	OFIS	cmg	ICP-AES; ICP-MS	-64,32559827	-12,2014551	Sirgas 2000
CM-17	OFIS	medium-grained	ICP-AES; ICP-MS	-64,32031587	-12,1957087	Sirgas 2000
CM-18	OFIS	cmg	ICP-AES; ICP-MS; EPMA	-64,33983102	-12,18750115	Sirgas 2000
CM-20	OFIS	-	ICP-AES; ICP-MS; EPMA	-64,34865287	-12,18598623	Sirgas 2000
CM-22	OFIS	trachyte dyke	ICP-AES; ICP-MS	-64,2946742	-12,21370933	Sirgas 2000
CM-25	SDIS	-	ICP-AES; ICP-MS	-64,33026796	-12,22230513	Sirgas 2000
CM-28	OFIS	cmg - fmg	ICP-AES; ICP-MS; EPMA	-64,27716137	-12,22603494	Sirgas 2000
CM-31	OFIS	fmg	ICP-AES; ICP-MS; EPMA; WDS	-64,27416325	-12,22303681	Sirgas 2000
CM-33	OFIS	fmg	ICP-AES; ICP-MS	-64,27492468	-12,21865861	Sirgas 2000
CM-39	OFIS	cmg	ICP-AES; ICP-MS; EPMA	-64,3559715	-12,19839274	Sirgas 2000
CM-40	CMIS	-	ICP-AES; ICP-MS	-64,30290714	-12,25212573	Sirgas 2000